

AD_____

Award Number: W81XWH-06-1-0332

TITLE: Decreased Expression of the Early Mitotic Gene, CHFR, Contributes to the Acquisition of Breast Cancer Phenotypes

PRINCIPAL INVESTIGATOR: Lisa Marie Privette

CONTRACTING ORGANIZATION: University of Michigan
Ann Arbor, MI 48109

REPORT DATE: March 2008

TYPE OF REPORT: Annual

PREPARED FOR: U.S. Army Medical Research and Materiel Command
Fort Detrick, Maryland 21702-5012

DISTRIBUTION STATEMENT: Approved for Public Release;
Distribution Unlimited

The views, opinions and/or findings contained in this report are those of the author(s) and should not be construed as an official Department of the Army position, policy or decision unless so designated by other documentation.

REPORT DOCUMENTATION PAGE				Form Approved OMB No. 0704-0188	
Public reporting burden for this collection of information is estimated to average 1 hour per response, including the time for reviewing instructions, searching existing data sources, gathering and maintaining the data needed, and completing and reviewing this collection of information. Send comments regarding this burden estimate or any other aspect of this collection of information, including suggestions for reducing this burden to Department of Defense, Washington Headquarters Services, Directorate for Information Operations and Reports (0704-0188), 1215 Jefferson Davis Highway, Suite 1204, Arlington, VA 22202-4302. Respondents should be aware that notwithstanding any other provision of law, no person shall be subject to any penalty for failing to comply with a collection of information if it does not display a currently valid OMB control number. PLEASE DO NOT RETURN YOUR FORM TO THE ABOVE ADDRESS.					
1. REPORT DATE (DD-MM-YYYY) 01-03-2008		2. REPORT TYPE Annual		3. DATES COVERED (From - To) 06 FEB 2007 - 05 FEB 2008	
4. TITLE AND SUBTITLE Decreased Expression of the Early Mitotic Gene, CHFR, Contributes to the Acquisition of Breast Cancer Phenotypes				5a. CONTRACT NUMBER	
				5b. GRANT NUMBER W81XWH-06-1-0332	
				5c. PROGRAM ELEMENT NUMBER	
6. AUTHOR(S) Lisa Marie Privette E-Mail: Imprivet@umich.edu				5d. PROJECT NUMBER	
				5e. TASK NUMBER	
				5f. WORK UNIT NUMBER	
7. PERFORMING ORGANIZATION NAME(S) AND ADDRESS(ES) University of Michigan Ann Arbor, MI 48109				8. PERFORMING ORGANIZATION REPORT NUMBER	
9. SPONSORING / MONITORING AGENCY NAME(S) AND ADDRESS(ES) U.S. Army Medical Research and Materiel Command Fort Detrick, Maryland 21702-5012				10. SPONSOR/MONITOR'S ACRONYM(S)	
				11. SPONSOR/MONITOR'S REPORT NUMBER(S)	
12. DISTRIBUTION / AVAILABILITY STATEMENT Approved for Public Release; Distribution Unlimited					
13. SUPPLEMENTARY NOTES					
14. ABSTRACT CHFR is an E3 ubiquitin ligase that reportedly delays mitosis in response to microtubule-targeting drugs (i.e. nocodazole and taxanes). Loss of CHFR mRNA expression has been reported in many cancers, including breast cancer, but the relevance of this to tumorigenesis remains unknown. The purpose of this study was to determine if CHFR was biologically relevant to breast cancer characteristics, progression, and genomic stability. As previously reported, nearly 40% of breast cancer show decreased CHFR expression compared to normal cells and tissues and the loss of CHFR expression by RNAi in cell culture models leads to the acquisition of several tumorigenic phenotypes. In particular, MCF10A IHMEC cells transfected with CHFR siRNA, became aneuploid and were analyzed for chromosome segregation defects. We observed increased aneuploidy, misaligned metaphase chromosomes, anaphase bridges, multi-polar condensed spindles, multi-nucleated cells, and mislocalization of the mitotic spindle checkpoint proteins MAD2 and BUBR1. CHFR was found to interact with three crucial mitosis proteins, including MAD2 and Aurora A where CHFR loss led to Aurora A oncoprotein over-expression, but no change in MAD2 expression. α -tubulin was identified as a novel target for CHFR-mediated ubiquitination after nocodazole treatment and decreased CHFR increased acetylated α -tubulin, a mitotic spindle protein implicated in cellular response to taxane treatment. These data indicate that CHFR has tumor suppressive qualities and may be a biomarker for taxane chemo-responsiveness. CHFR also has a previously unrecognized role as a regulator of genomic stability. CHFR may be one of the few proteins that can control the cell cycle, chemotherapeutic response, and genomic stability - processes that go awry in breast cancer.					
15. SUBJECT TERMS Cell cycle, mitotic checkpoints, CHFR, chemotherapeutic response, and tumorigenesis					
16. SECURITY CLASSIFICATION OF:			17. LIMITATION OF ABSTRACT	18. NUMBER OF PAGES	19a. NAME OF RESPONSIBLE PERSON
a. REPORT	b. ABSTRACT	c. THIS PAGE			USAMRMC
U	U	U	UU	61	19b. TELEPHONE NUMBER (include area code)

Table of Contents

	<u>Page</u>
Introduction.....	1
Report Body.....	1
Key Research Accomplishments.....	6
Reportable Outcomes.....	7
Training Progress.....	7
Conclusion.....	8
References.....	9
Appendices	
Appendix 1 (<i>Cancer Research</i>).....	11
Appendix 2 (paper in preparation).....	22
Appendix 3 (<i>Curriculum vitae</i>).....	54

Introduction:

CHFR (Checkpoint with FHA and Ring Finger) has been reported to mediate a delay in the progression of mitosis, during prophase, in response to microtubule stress. Examples of microtubule stress include exposure to the chemotherapeutic drug Taxol, which is often used to treat breast cancer patients, or nocadazole. As a potential regulator of cell cycle progression and drug response, CHFR naturally becomes an interesting target for study in breast cancer. Little is known about the molecular functions and signaling pathways that CHFR mediates. However, mRNA of *CHFR* has been reported frequently to show decreased or lost gene expression in cancer cells when compared to normal cells from the same tissue, but the relevance of this for tumorigenesis had remained unclear. The purpose of this study was to characterize the role of CHFR in breast cancer tumorigenesis using both cultured breast cancer cell lines and primary breast cancers from patients. In particular, the research presented here analyzed the expression of CHFR protein in cell lines and primary tumors and then tried to correlate protein expression with clinical and pathological information from primary samples. In addition, cell culture models were used to determine if changing *CHFR* expression would result in the cells becoming more like cancer cells instead of normal mammary epithelia. Further work has identified novel CHFR-interacting proteins and a role for CHFR in regulating genomic stability, potentially through the mitotic spindle assembly checkpoint.

Report:

Task 1: Determine if CHFR protein expression is decreased or lost in breast cancers and if its expression has prognostic value using both mammary epithelial cell lines and primary matched normal and tumor tissues. (Months 1-15)

Outstanding progress has been made on Task 1, such that this task is almost entirely complete. Results from these important studies suggest that the loss of CHFR expression is associated with other clinical variables as described below. Some of this work was published in the July 1, 2007 issue of Cancer Research (appendix 1).

Task 1a: Use Western blot analysis with a newly developed polyclonal antibody to analyze CHFR protein expression in approximately 30 immortalized and transformed mammary epithelial cell lines (months 1-4).

Since the last reporting period, I have repeated this aim due to reviewers' concerns about over-exposure and uneven loading in the previously presented data. Western blotting was performed using whole cell lysates from a panel of unsynchronized breast cancer cells and immortalized ("normal") human mammary epithelial cells (HMECs). Initially, a custom-made polyclonal antibody was used, but has since been replaced by a commercially available monoclonal antibody (Abnova Corp.) Using this antibody for Western blotting, I found that 41% of breast cancer cell lines had CHFR expression lower than that observed in the HMEC lines (Fig. 1A, appendix 1). This task is now completed.

Task 1b: Perform immunohistochemistry on matched normal and breast cancer tissues obtained from patient samples from the University of Michigan (months 4-12).

I have obtained matched normal and breast cancer tissues from patients at the University of Michigan. Though no difference was detected between the normal and cancer tissues by immunohistochemistry with the monoclonal CHFR antibody, this is likely due to the small sample size (N=3). I hope to obtain additional samples in the coming months. However, I did find that CHFR is strongly expressed in the epithelial cells lining the ducts of the mammary gland in all three patient samples of normal breast tissue, as expected (Figure 1B, appendix 1).

Task 1c and 1d: Conduct tissue microarrays to detect CHFR expression across a range of tumor grades and stages (months 8-14). Perform statistical analysis (Fisher's exact test and Chi square tests) to determine if the loss of CHFR expression is correlated with different stages of tumorigenesis (months 14-15).

The results of this task were described in the last annual report. Please see the manuscript included in the appendix 1 for details on methods and results. This task has been completed on schedule. In summary, 36% of primary invasive breast cancers were completely negative for CHFR expression. Negative CHFR expression strongly correlated with large tumor size and there was a trend towards the absence of CHFR expression correlating with estrogen receptor negative (ER-) status in primary invasive breast cancers (Fig. 1C and 1D, appendix 1).

Task 2: Examine if CHFR expression correlates with cancer phenotypes in vitro (Months 12-25)

We are excited about the significant progress I have made on this task. Many of the findings described in last year's annual report were very interesting and indicated several novel roles for CHFR in regulating breast cancer tumorigenesis in cell culture models. The bulk of this work was published in the July 1, 2007 issue of Cancer Research (appendix 1). This past year has focused on elucidating the role of CHFR in regulating genomic stability, which was part of task 2C, described below.

Task 2a: Design a retroviral vector that will have controlled, inducible expression of CHFR, infect breast cancer cell lines (Hs578t and BT20) with the retrovirus carrying the construct, and select for stable transformants (months 12-17)

Great progress has been made in completing this aim. I have cloned a green fluorescent protein (GFP)-tagged CHFR construct into a tetracycline-regulated expression system, in which CHFR expression can be controlled, turned on or off within the cell, using a tetracycline responsive promoter. This will allow us to correlate better the amount of CHFR with cellular phenotypes. The GFP tag also will allow me to perform live cell imaging so that I can visualize the cells and their behavior, and the localization of CHFR, in real time. In addition, creating this gene construct will make it easier to determine what happens to a mammary epithelial cell, or breast cancer cell, when CHFR expression is re-introduced since it has proven extremely difficult to over-express CHFR in all breast cells independent of the method used; high expression appears to be toxic. This system has been transfected into the MCF10A IHMEC cell line and is currently under selection to identify positive clones, after which tetracycline expression will be titrated to determine optimal conditions for GFP:CHFR expression. This aim has taken longer than expected due to low transfection efficiency of the MCF10A cell line. The subsequent phenotypic analyses will require approximately four to six months to accomplish, at least.

However, as described last year, evidence using an unregulated CHFR expression construct indicated that expression at physiological levels in a breast cancer cell line that does

not normally express CHFR, Hs578T, can reverse some of the tumorigenic phenotypes of that cell, particularly invasive potential and motility (Fig. 5A-D, appendix 1). This was the only breast cancer cell line to date that is capable of expressing CHFR after retroviral transduction of a full-length cDNA encoding CHFR. We think more significant results will be evident if the amount of CHFR that is overexpressed can be titrated to prevent cellular toxicity, as described above.

Task 2b: Design a retroviral vector that will express a siRNA construct targeted against CHFR to decrease CHFR expression in “normal” immortalized mammary epithelial cell lines (MCF10A and HPV 1-30). Transduce cell lines with the retrovirus construct and select for stable clones (months 12-17).

This task was accomplished and described in last year’s annual report. The shRNA expression construct described here was used to characterize the effects of decreased CHFR expression in immortalized human mammary epithelial cells, as described below in task 2c. Results for this task are described in Fig. 2A, appendix 1.

Task 2c: Analyze transduced cell lines (see above) for changes in cancer-related phenotypes: (1) foci formation, (2) Matrigel invasion assay, (3) migration assay, (4) changes in growth rate, (5) changes in mitotic index (ratio of cells undergoing mitosis at a given timepoint), (6) alterations in genomic stability/ploidy status, and (7) response to treatment with nocodazole, and paclitaxel (months 17-25)

I tested the cell lines with drastically less CHFR to determine if their characteristics had changed to look more like breast cancer cells instead of normal epithelial cells. I tested both of the cell lines, HPV4-12 and MCF10A, using several cell culture-based assay.

As described last year, it was determined that cells with stably decreased CHFR expression by shRNA grew faster than their untransduced parental counterparts and the negative controls, which had a non-targeting shRNA construct (Fig. 2B, appendix 1). This past year, I analyzed this phenotype more closely and tested the cells to determine if the checkpoint function has been compromised due to decreased CHFR expression. One of the likely contributing factors to the increased growth rates was that cells transduced with CHFR shRNA had a much higher mitotic index as evidenced by an increased frequency of phosphorylation on histone H3 on residue Ser28 (which is a common mitotic marker; Fig. 3C). This occurred even without the presence of microtubule poisons such as nocodazole, and indicated that more cells were actively in mitosis in CHFR knockdown cells. However, further work is required in the coming months to determine if this is due to altered timing of mitotic entry or a prolonged amount of time within mitosis due to the stress of having lost CHFR expression. Using the phosphorylation of histone H3 on residue Ser28 as a marker of a cell progressing through the CHFR-mediated early mitotic checkpoint¹, I was also able to confirm that decreased CHFR expression caused an impaired checkpoint, leading to more late mitotic cells following treatment with microtubule poisons such as nocodazole (Fig. 3C right panel, appendix 1).

As described in last year’s annual report, the cells with decreased CHFR expression by RNAi had acquired many tumorigenic phenotypes compared to control cells. Briefly, the cells with either a permanent or a temporary loss of CHFR, also became more invasive, using a Matrigel invasion assay, and more motile when compared to controls (Fig. 3A and 3B, appendix 1). Intriguingly, both cell lines, HPV4-12 and MCF10A, acquired increased numbers of misshapen nucleoli when CHFR was absent; this phenotype strongly correlates with a poor

patient prognosis when it is observed in primary cancers (Fig. 4A and 4B, appendix 1). In addition, only the MCF10A cell line underwent a morphology change so that it appeared mesenchymal instead of epithelial when CHFR was absent (Fig. 4C, appendix 1). This cellular transition is sometimes observed in primary breast cancers. Finally, cytogenetic analysis revealed that both HPV4-12 and MCF10A cells became more aneuploid without CHFR, indicating that CHFR is important in maintaining genomic stability in normal cells (Fig. 6A and 6B, appendix 1, Fig. 1A-C, appendix 2). Together, these results suggest a critically important role for CHFR expression in mammary tumorigenesis. Details on the methods and results from these experiments are included in the text of the manuscript included in the appendix.

One of the more significant findings from this task that has been determined in the past year was that the HPV4-12 cells with decreased CHFR expression were able to grow more colonies in soft agar compared to negative controls (Fig. 4D, appendix 1. This indicated that the cells had potentially become transformed).

In the past year, the phenotype of genomic instability was analyzed further to determine how cells without CHFR improperly separate their chromosomes during mitosis. MCF10A cells transiently transfected with CHFR siRNA became more aneuploid within 72 hours, indicating that the aneuploidy observed in the stable shRNA-expressing constructs was not due to culture conditions or clonal expansion (Fig. 1D-F, appendix 2). To test for the cause of this rapid onset of increased aneuploidy, I used immunofluorescence to visualize chromosome segregation during mitosis. I have found that the transient loss of CHFR expression by siRNA in MCF10A cells leads to four mitotic defects: (1) mis-aligned chromosomes at the metaphase plate, (2) poorly formed, multi-polar mitotic spindles, suggesting centrosome amplification, (3) lagging anaphase chromosomes, and (4) bi-nucleated cells indicating failed cytokinesis (Fig. 2A-C and 2G, appendix 2). Importantly, I also found that the localization of the key mitotic spindle proteins, MAD2 and BUBR1, are mislocalized early in mitosis in CHFR knockdown cells compared to negative controls (Fig. 2D and 2E, appendix 2). This indicated that the mitotic spindle assembly checkpoint was impaired, suggesting that CHFR may participate in the regulation of more than one mitotic checkpoint. In the next six to twelve months, this phenotype will be studied further, including the use of live cell imaging to analyze chromosome segregation and mitotic spindle formation in real time so that the specific mitotic defects occurring in CHFR knockdown cells can be described better.

This past year, I also used this cell culture model to determine if decreased CHFR expression altered cellular sensitivity to microtubule-targeting poisons, such as nocodazole and the chemotherapeutic drug paclitaxel (Taxol). I used annexin V staining of the cell membrane as an indicator of apoptosis followed by flow cytometry to determine if cells without CHFR undergo more or less cell death in response to drug treatment². Importantly, I found that decreasing CHFR expression by RNAi in MCF10A cells caused an enhanced sensitivity (i.e.: increased apoptotic response) to nocodazole and paclitaxel, indicating that CHFR may serve as an important biomarker for chemotherapeutic response to taxane treatment (Fig. 2D, appendix 1). Interestingly, HPV4-12 cells, which have impaired p53 and pRb function due to immortalization with the human papilloma virus (HPV) E6 and E7 proteins, which had decreased CHFR expression by RNAi did not have an altered apoptotic response. From this, I hypothesize that the p53 pathway may be an important regulator of the apoptotic response to microtubule-targeting drugs, and that the expression of CHFR may negatively regulate this pathway. However, a great deal of future work is required to test this hypothesis.

Task 3: Characterize CHFR as a cell cycle checkpoint protein in mammary epithelial cells (Months 24-36)

Though work on this task has just recently begun, initial findings are promising and significant progress has been made in a relatively short period.

Task 3a: Perform Western blot and immuno-fluorescence to determine expression and cellular localization of CHFR at different stages of the cell cycle in mammary epithelial cell lines (months 24-26).

The experiments for this task are currently underway. As described in Task 2a, I have cloned a GFP-CHFR fusion construct under the control of a tetracycline-regulated promoter. This will allow easy detection of CHFR localization at different stages of the cell cycle by using live-cell imaging to determine if CHFR changes localization in response to cell cycle stage or drug treatment. I am working closely with our Live Cell Imaging Core in developing reliable and robust experiments.

I have also synchronized four breast cancer cell lines (BT20, Cal51, Hs578T, and T47D), which showed low or inconsistent CHFR expression in previous experiments, and two IHMEC lines (MCF10A and HPV4-12) in the G1/S phases of the cell cycle by a double-thymidine block. Cells and protein lysates were collected during a time-course from the release of the double-thymidine block to monitor CHFR expression during the cell cycle. Cells were analyzed by flow cytometry with propidium iodide staining to determine cell cycle stage while the lysates were tested for CHFR expression by Western blotting. From the two IHMEC cell lines, I have initially found that CHFR is highly expressed in the S and G2/M phases of the cell cycle, though it may be lower in the G1 phase. In addition, three of the four breast cancer cell lines showed deregulated CHFR protein expression. Further experiments are underway to elucidate further the possibility that CHFR expression is cell cycle-regulated.

Task 3b: Find novel interacting partners with CHFR using GST pull-down and confirm with immunoprecipitation experiments (months 26-36).

I have begun to perform these experiments and have found, by both GST pull-downs and co-immunoprecipitation experiments that CHFR can interact with the α -tubulin subunit of the microtubules, which agrees with the fact that CHFR can regulate the early mitotic cell cycle delay in response to microtubule stress. However, I have been unable to find an interaction between CHFR and either β - or γ -tubulin. MCF10A cells transfected with or without CHFR siRNA and treated with the proteasome inhibitor MG132 with or without simultaneous treatment with nocodazole were subjected to immunoprecipitation for α -tubulin. These samples were then tested by Western blotting for the ubiquitination of α -tubulin. With this method, I have found that CHFR can ubiquitinate α -tubulin during treatment with the microtubule poison nocodazole and that decreased CHFR expression not only leads to a slight increase in α -tubulin levels, but also causes a nearly 2-fold increase in acetylated α -tubulin, which is a primary component of the mitotic spindle (Fig. 4, appendix 2).

By performing co-immunoprecipitation experiments, I have also confirmed that CHFR can interact with the key mitotic kinase Aurora A, which was previously published³, and that decreased CHFR expression leads to Aurora A over-expression (Fig. 3, appendix 2). Finally, I have also identified a novel interaction between CHFR and the important spindle checkpoint

protein MAD2 (Fig. 2F, appendix 2). This finding supports the findings presented in Task 2c, in which decreased CHFR expression by siRNA caused MAD2 mislocalization. This data is particularly interesting because it is an important clue in determining how CHFR regulates genomic stability and implicates CHFR in regulating *two* mitotic checkpoints – the early microtubule-stress induced checkpoint in prophase, and the widely known spindle assembly checkpoint. Experiments are currently in progress to determine if CHFR can regulate the ubiquitination of MAD2 or the interaction between MAD2 and cdc20.

Task 3c: Test cellular responses of cells with and without CHFR to other chemotherapeutic drugs (months 30-36).

The cells to be used for this task were generated for Task 2, described above. These experiments are still being planned and will be addressed in the next year.

Key Research Accomplishments:

Work on this project over the past year has lead to noteworthy novel results that highlight the relevance of CHFR expression to breast cancer. Specifically, I have found that:

- Normal mammary epithelium stains strongly for CHFR expression by immunohistochemistry.
- I have cloned a GFP-CHFR fusion construct under the control of a tetracycline-regulated promoter (pcDNA4/TO-GFP:CHFR to be transfected with pcDNA6/TR) and I am in the process of transfecting MCF10A cells with these plasmids. This construct will be used to analyze the effects of CHFR over-expression and to visualize CHFR localization using live-cell imaging.
- IHMEC lines with stably decreased CHFR expression by shRNA show:
 - Increased phosphorylation of histone H3 at Ser28, indicating a higher mitotic index and an impaired checkpoint in response to microtubule poisons
 - Colony formation of HPV4-12 IHMEC cells in soft agar, suggesting cellular transformation
- MCF10A cells with transiently decreased CHFR expression by siRNA show:
 - Increased sensitivity (apoptotic response) to nocodazole and paclitaxel in the MCF10A cell line
 - Rapid onset of aneuploidy
 - Four mitotic defects:
 - Misaligned metaphase chromosomes
 - Lagging anaphase chromosomes
 - Poorly formed, multi-polar mitotic spindles
 - Bi-nucleated giant cells
 - Mislocalization of the key mitotic checkpoint proteins MAD2 and BUBR1
 - Over-expression of α -tubulin and acetylated α -tubulin and Aurora A kinase

- The following CHFR interacting proteins were identified:
 - α -tubulin (and ubiquitinated by CHFR)
 - Aurora A kinase
 - MAD2

Reportable Outcomes:

Degrees Awarded:

University of Michigan's Rackham Graduate School: Ph.D. in the Department of Human Genetics. Oral Dissertation Defense: February 1, 2008. Degree Conferred: April 25, 2008

Manuscripts:

Privette, L.M. and Petty, E.M., "CHFR: a novel mitotic checkpoint protein and regulator of tumorigenesis," invited review, *in preparation* for *Translational Oncology*

Privette, L.M., Weier, J.F., Nguyen, H.N., Yu, X. Petty, E.M., "Loss of CHFR expression in mammary epithelial cells causes genomic instability" *in revision* for *Neoplasia*

Privette, L.M., Gonzalez, M.E., Ding, L., Kleer, C.G., Petty, E.M., "Altered expression of the early mitotic checkpoint gene, CHFR, in breast cancers: Implications for tumor suppression," *Cancer Res.* 2007; 67: (13). July 1, 2007

Presentations:

National Meetings:

Poster: *L.M. Privette* and E.M. Petty, "Loss of CHFR potentiates the development of oncogenic phenotypes and creates genomic instability in mammary epithelial cells," "Mechanisms and Models of Cancer" meeting, Salk Institute, La Jolla, CA, August 8-12, 2007

Local Meetings:

Posters:

University of Michigan (UM) Cancer Center Research Symposium,
November 16, 2007

UM Department of Human Genetics Annual Symposium, May 17, 2007

UM Genetics Training Grant Annual Symposium, May 7, 2007

UM Department of Internal Medicine Annual Symposium, May 4, 2007

Oral Presentation:

UM Genetics Training Grant Student Seminar, January 9, 2007

Training Progress:

- Completed all coursework and independent research credits for the Ph.D. degree from the University of Michigan

- Director of Genetics Education for the University of Michigan's Summer Science Academy summer camp for underprivileged high school students
- At least one meeting weekly with mentor, Elizabeth M. Petty, M.D., and monthly meetings with co-mentor, Thomas Glover, PhD.
- Semi-annual meetings with thesis committee to discuss progress: Elizabeth M. Petty, Thomas Glover, Diane Robins, Celina G. Kleer, and Mats Ljungman
- Attended nearly every seminar in the "Cancer Center Grand Rounds" series
- Attended nearly every seminar in the "Hematology/Oncology Grand Rounds" series
- Attended the annual Department of Human Genetics Retreat
- Attended the national "Mechanisms and Models of Cancer" meeting, Salk Institute, La Jolla, CA, August 8-12, 2007
- Attended twice-monthly "Cell Cycle Checkpoints" journal club
- Attended weekly research seminars and journal club meetings in the Department of Human Genetics
- Collaborated with breast cancer pathologists Celina Kleer and Thomas Giordano
- Learned/improved the following techniques: mammary epithelial and breast cancer cell culture and associated techniques, immunofluorescence, co-immunoprecipitation, immunohistochemistry, flow cytometry, many PCR-based techniques, and Western blotting

Conclusion:

The first two tasks from the statement of work are nearly complete and the experiments described in the third task are underway, and much progress has been made to finish that aim. The works described in the above tasks have been published in *Cancer Research* and are in preparation for publication in another journal.

The data presented here shows that 41% of cell lines have lost protein expression and that 36% of primary invasive cancers are negative for CHFR; this agrees with the preliminary findings presented in the original proposal in which many breast cancer cell lines showed low or lost *CHFR* mRNA expression. In primary breast cancers, the absence of CHFR staining strongly correlated with a small (>2cm) tumor size and there was a trend towards an association with estrogen receptor-negative status. In addition, preliminary data from the original proposal indicated that breast cancer cell lines with low CHFR expression tended to have a high mitotic index. This is supported by our evidence that showed IHMECs with lowered CHFR expression had a higher percentage of cells that bypassed the CHFR checkpoint and entered mitosis, as evidence by phosphor-H3-Ser28 staining by immunofluorescence. Strong proof that CHFR has important tumor suppressive qualities in breast cancer comes from the studies in task two from the statement of work, which described the phenotypic changes that a fairly normal cells undergoes when it experiences an extreme decrease (near loss) of CHFR expression. Two different IHMEC lines, using two different methods to decrease expression, revealed that cells with a significantly lowered amount of CHFR began to grow faster, became more invasive and motile, underwent changes in nucleoli numbers and cellular morphology, could form colonies in soft agar, and became aneuploid. All of these changes mimic those that a normal cell undergoes in the patient to develop into a tumor. It was incredibly interesting to realize that CHFR loss had such a great impact on invasive potential and motility *in vitro*; this indicated that CHFR may be

important in regulating tumor metastasis in the patient, a finding that had never before been associated with CHFR.

In addition, cell culture models of CHFR loss indicate that it may be a biomarker for chemotherapeutic response to taxanes; however, the differential response between the two IHMEC lines indicates that the genetic background of the cell also influences this increase in apoptotic response. It is interesting to note that there was a trend towards negative CHFR expression being associated with negative estrogen receptor (ER) expression, which has clinical and treatment implications. Estrogen receptor-negative, and therefore possibly CHFR-negative, breast cancers are known to be receptive to taxane treatment while ER-positive (and potentially CHFR-positive) cells are notoriously resistant to taxane treatment⁴⁻⁶. This is further supported by my finding that CHFR can ubiquitinate α -tubulin when the cells are exposed to the microtubule poison nocodazole. This may be one mechanism for how CHFR mediates the cellular response to taxanes and other microtubule-targeting drugs. Perhaps CHFR is needed to ubiquitinate tubulins that have been damaged by the drugs in order to remove them so that they can be replaced by un-poisoned tubulin proteins to reform the microtubules.

New evidence described this year indicates that CHFR may function in multiple mitotic checkpoints: the early microtubule-stress checkpoint in prophase and the later spindle assembly checkpoint. I have found that the loss of CHFR leads to four mitotic defects including misaligned metaphase chromosomes, lagging anaphase chromosomes, poorly formed multi-polar spindles, and binucleated giant cells. All of these phenotypes suggest a defect in the spindle assembly checkpoint, which was further supported by the finding that the key mitotic spindle checkpoint proteins, MAD2 and BUBR1, were mislocalized in cells with decreased CHFR expression. Finally, I have found that CHFR can interact with, and in some cases ubiquitinate, several key mitotic proteins including Aurora A kinase, the α -tubulin component of the mitotic spindle, and the spindle checkpoint protein MAD2. Further work is in progress to explore the function of the MAD2/CHFR interaction. The relatively high frequency of down-regulated CHFR expression in breast cancers may be one explanation as to why the occurrence of aneuploidy is so high in breast cancers, but the mutation or deregulation of other spindle checkpoint proteins is rare⁷⁻⁹.

The combination of initial evidence presented in the proposal with the new findings described here indicate that CHFR contributes significantly to maintaining genomic stability and normal cellular function and, more importantly, appears to have a great tumor suppressor function in mammary tissues.

References:

1. Crosio, C., *et al.* Mitotic Phosphorylation of Histone H3: Spatio-Temporal Regulation by Mammalian Aurora Kinases, *Mol. Cell. Biol.*, 2002, 22(3), 874-885
2. Vermes, I., Haanen, C., Steffens-Nakken, H., and Reutelingsperger C. A novel assay for apoptosis. Flow cytometric detection of phosphatidylserine expression on early apoptotic cells using fluorescein labelled Annexin V, *J Immunol. Methods*, 1995, 184(1):39-51

3. Yu, X, Minter-Dykhouse, K, Malureanu, L, Zhao, WM, Zhang, D, Merkle, CJ, Ward, IM, Saya, H, Fang, G, van Deursen, J, and Chen, J. Chfr is required for tumor suppression and Aurora A regulation. *Nat Genet.* 2005; 37: 401-406.
4. Berry, D. A., Cirrincione, C., Henderson, I. C., Citron, M. L., Budman, D. R., Goldstein, L. J., Martino, S., Perez, E. A., Muss, H. B., Norton, L., Hudis, C., and Winer, E. P. Estrogen-receptor status and outcomes of modern chemotherapy for patients with node-positive breast cancer. *Jama* 2006; 295: 1658-1667.
5. Poole, C. Adjuvant chemotherapy for early-stage breast cancer: the tAnGo trial. *Oncology (Williston Park)* 2004; 18: 23-26.
6. Sezgin, C., Karabulut, B., Uslu, R., Sanli, U. A., Goksel, G., Zekioglu, O., Ozdemir, N., and Goker, E. Potential predictive factors for response to weekly paclitaxel treatment in patients with metastatic breast cancer. *J Chemother* 2005; 17: 96-103.
7. Kops, GJ, Weaver, BA, and Cleveland, DW. On the road to cancer: aneuploidy and the mitotic checkpoint. *Nat Rev Cancer.* 2005; 5: 773-785.
8. Myrie, KA, Percy, MJ, Azim, JN, Neeley, CK, and Petty, EM. Mutation and expression analysis of human BUB1 and BUB1B in aneuploid breast cancer cell lines. *Cancer Lett.* 2000; 152: 193-199.
9. Percy, MJ, Myrie, KA, Neeley, CK, Azim, JN, Ethier, SP, and Petty, EM. Expression and mutational analyses of the human MAD2L1 gene in breast cancer cells. *Genes Chromosomes Cancer.* 2000; 29: 356-362.

Research Article

Altered Expression of the Early Mitotic Checkpoint Protein, CHFR, in Breast Cancers: Implications for Tumor Suppression

Lisa M. Privette,¹ Maria E. González,² Lei Ding,³ Celina G. Kleer,³ and Elizabeth M. Petty^{1,2}Departments of ¹Human Genetics, ²Internal Medicine, and ³Pathology, University of Michigan, Ann Arbor, Michigan

Abstract

Checkpoint with FHA and Ring Finger (CHFR) is hypothesized to mediate a delay in cell cycle progression early in mitosis in response to microtubule stress, independent of the spindle assembly checkpoint. As a potential regulator of cell cycle progression, CHFR naturally becomes an interesting target for understanding cancer cells. In recent years, there has been increasing evidence supporting the role of CHFR as a tumor suppressor, most of which report loss of expression, occasionally due to promoter hypermethylation, in cancers compared with patient-matched normal tissues. We studied both a panel of breast cancer cell lines as well as primary tissue samples from breast cancer patients to investigate CHFR as a relevant tumor suppressor in breast cancer and to determine whether CHFR expression was associated with clinical and pathologic variables. We report that 41% of cell lines and 36% of patient samples showed low or negative CHFR protein expression or staining. In addition, lack of CHFR detection was associated with increased tumor size and weakly correlated with estrogen receptor-negative tumors from patients. To study the effects of low CHFR expression *in vitro*, we stably expressed a short hairpin RNA construct targeting *CHFR* in two lines of immortalized human mammary epithelial cells. Notably, decreased CHFR expression resulted in the acquisition of many phenotypes associated with malignant progression, including accelerated growth rates, higher mitotic index, enhanced invasiveness, increased motility, greater aneuploidy, and amplified colony formation in soft agar, further supporting the role of CHFR as a tumor suppressor in breast cancer. [Cancer Res 2007;67(13):6064–74]

Introduction

Breast cancer, the second leading cause of cancer-related death among women in the United States, is often associated with defects in cell cycle checkpoint regulation. Checkpoint with FHA and Ring Finger (CHFR) is a checkpoint protein that reportedly initiates a cell cycle delay in response to microtubule stress during prophase in mitosis (1). This delay is thought to occur before chromosome condensation by excluding cyclin B1 from the nucleus (2). One form of microtubule stress is treatment with taxanes, such as nocodazole or paclitaxel (Taxol), a chemotherapeutic drug used for cancer patients, including those with breast cancer (3). Therefore, CHFR has been hypothesized to be a tumor suppressor with a

potential role as a biomarker for chemotherapeutic response to Taxol (4, 5). Many reports have noted that cancer cells that have lost *CHFR* expression are more likely to undergo apoptosis in response to microtubule poisons, which strongly supports this hypothesis (1, 5–7). The molecular mechanism by which CHFR initiates a cell cycle arrest is debated, although evidence implicates the p38/mitogen-activated protein kinase pathway, an Aurora A interaction, and/or through regulation of PLK-1 (8–11).

There is evidence that *CHFR* may function, in part, as a tumor suppressor gene. Most notably, several groups have shown that *CHFR* mRNA expression is lost or decreased in primary tumors and cancer cell lines when compared with matched normal tissues and cells. The best characterized means of expression loss is promoter hypermethylation, which occurs in a subset of tumors and cell lines and the frequency of which seems to be dependent on the tissue of origin (4, 5, 12–20). Further support that *CHFR* may mediate tumorigenesis is that its chromosomal location, 12q24, is a site for allelic imbalance and chromosome rearrangements in several types of cancer (21–25). In addition, Yu et al. (11) published recently their description of a *Chfr* knockout mouse. The null mice were prone to developing tumors and mouse embryonic fibroblasts were aneuploid, suggesting a role for CHFR in genomic stability. However, to date, there has been little functional evidence describing *CHFR* as a tumor suppressor in a human model system.

To characterize the role of CHFR in breast cancer, we used both cultured breast cell lines and primary patient samples. We assessed the expression of CHFR protein and mRNA in a panel of breast cancer cell (BCC) lines and found that expression is low or absent in many of them when compared with immortalized human mammary epithelial cells (IHMEC). Analysis of a tissue microarray (TMA) composed of primary invasive breast cancer samples indicated that a significant number of patient samples showed negative or weak CHFR protein staining by immunohistochemistry and that CHFR staining was inversely correlated with tumor size. In view of this evidence that CHFR may be a tumor suppressor, we mimicked cellular loss of expression via stable short hairpin RNA (shRNA) and transient small interfering RNA (siRNA) targeting CHFR in two IHMEC lines. This decrease in expression led to the acquisition of many phenotypes associated with malignant progression.

Materials and Methods

Cell culture. Most cell lines were obtained from the American Type Culture Collection and grown under recommended conditions. SUM1315, SUM102, SUM190, SUM159, SUM149, SUM52, SUM185, SUM225, and SUM229 and the human papilloma virus (HPV)-immortalized series of nontumorigenic mammary cell lines were developed and provided by S.P. Ethier, Karmanos Cancer Institute, Wayne State University, Detroit, MI (now available from Asterand), and cultured according to specified conditions (26). A detailed description of relevant cell line information, including origins and hormone receptor status, has been compiled by Neve et al. (27). Please see Supplementary Table S1 for a brief description of the three cell lines predominantly used in this report.

Note: Supplementary data for this article are available at Cancer Research Online (<http://cancerres.aacrjournals.org/>).

Requests for reprints: Elizabeth M. Petty, Departments of Human Genetics and Internal Medicine, University of Michigan, 5220A MSRBIII, 1150 West Medical Center Drive, Ann Arbor, MI 48109-0638. E-mail: epetty@umich.edu.

©2007 American Association for Cancer Research.

doi:10.1158/0008-5472.CAN-06-4109

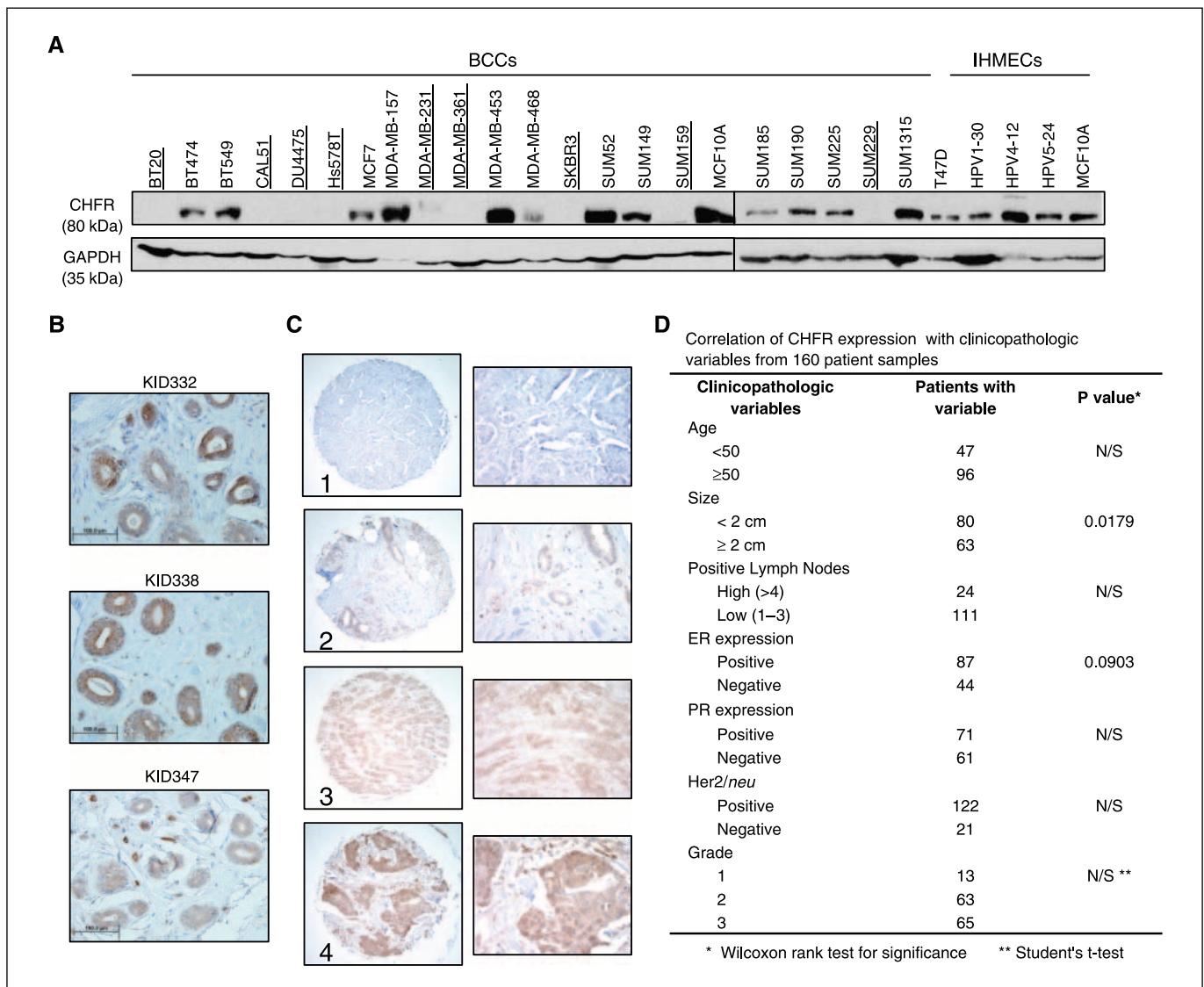


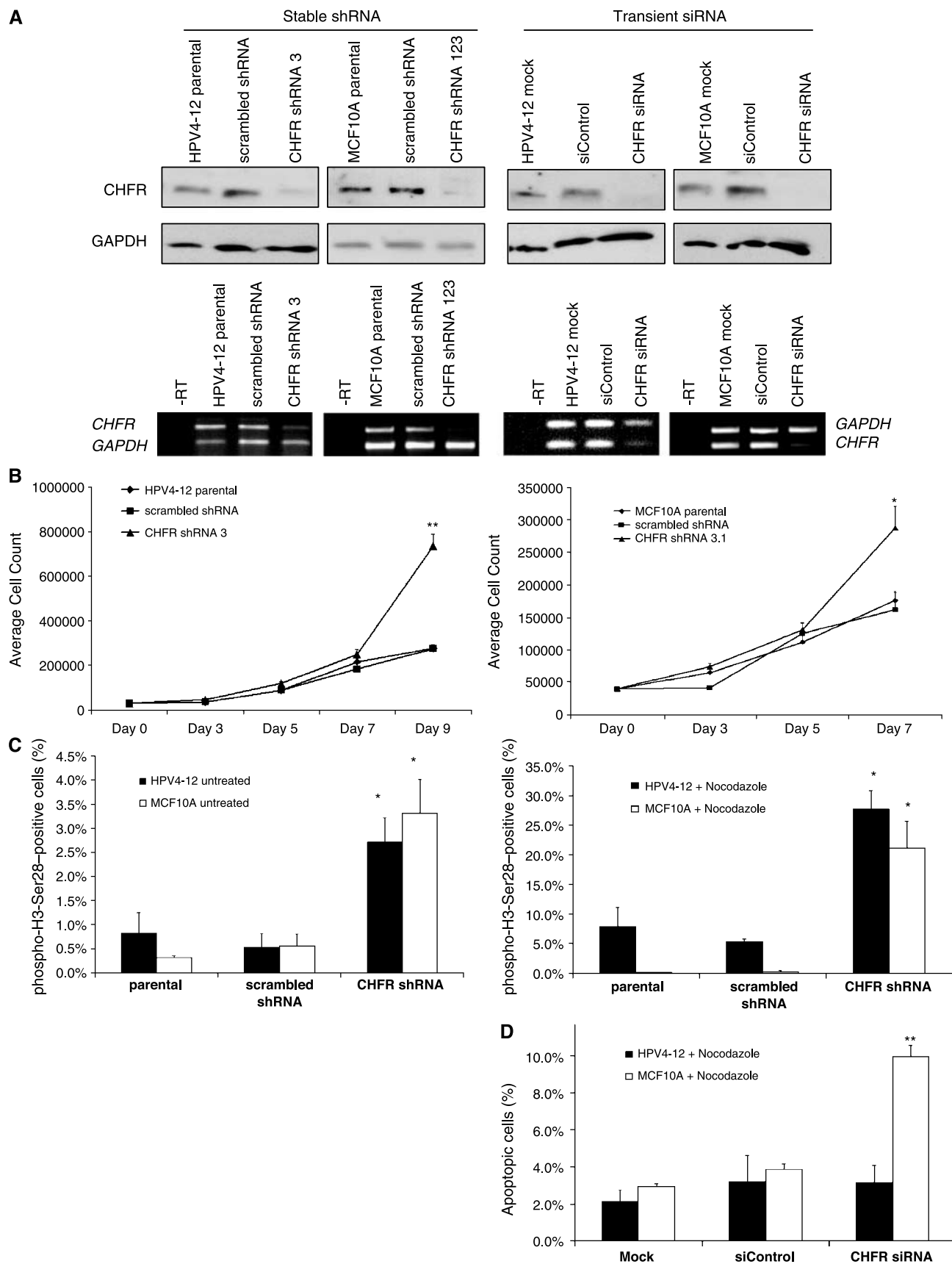
Figure 1. CHFR protein expression is low or lost in a subset of BCCs and primary tumors when compared with “normal” IHMECs and breast tissue, and positive expression correlates with small tumor size *in vivo*. **A**, Western blot analysis using a monoclonal CHFR antibody reveals that 9 of 22 (41%, underlined) asynchronous BCC lines, or BCCs, at 70% to 80% confluence have low CHFR expression compared with the lowest level of expression observed among four asynchronous IHMECs. To control for loading, an antibody against GAPDH was used (*bottom*). A composite image of two separate Western blots. Whole-cell lysate from the MCF10A IHMEC line was used as a control on both blots in the composite image. **B**, immunohistochemistry using the monoclonal CHFR antibody showed prominent staining in the mammary gland epithelia of normal primary breast samples. Representative examples are indicated by three separate patient tissues: KID332, KID338, and KID347. **C**, immunohistochemistry using a mAb against CHFR on primary invasive breast cancers from a TMA shows a range of CHFR expression. Intensity of CHFR staining ranged from negative (1) to weak (2), moderate (3), and strong (4). Magnifications, $\times 10$ (*left*) and $\times 40$ (*right*) from sections of the adjacent image. **D**, statistical analyses of clinicopathologic characteristics from 142 primary invasive breast carcinoma samples indicate that positive CHFR expression correlates strongly with small (<2 cm) tumor size and has a weaker association with ER positive (ER+) status. A sample was determined to be positive for CHFR if its staining intensity scored at a 2, 3, or 4. *P* values were calculated using the Wilcoxon rank test, except for tumor grade (*) for which the *P* value was calculated using Student's *t* test.

For retroviral transduction, PT67 packaging cells were transfected using Eugene 6 with 10.0 μ g pRNA-H1.1/Hygro vector (GenScript Corp.) containing either a scrambled sequence or a CHFR shRNA construct targeting nucleotides 324 to 344, 1491 to 1511, or 2497 to 2517 (accession no. AF170724). We used the pLPCX retroviral vector for overexpression of full-length CHFR in Hs578T cells (Clontech Laboratories). Virus was collected after 48 h and purified with a 0.45-micron filter. Equal parts of retrovirus-containing media and normal growth media were added to 1×10^6 cells. Fresh medium was added 24 h later and selection with 20.0 μ g/mL hygromycin (pRNAH1.1) or 1.5 μ g/mL puromycin (pLPCX) began 48 h after infection. The resulting polyclonal cell population stably expressing the CHFR construct(s) was subsequently used for experimentation. MCF10A cells were transduced with all three shRNA constructs, whereas HPV4-12

cells were transduced with the shRNA construct targeting nucleotides 324 to 344 to achieve maximum knockdown.

Transient transfection of siControl or a pool of four siRNAs targeting CHFR (siGENOME, Dharmacon RNA Technologies) was done according to the manufacturer's instructions. HPV4-12 cells were transfected using Dharmafect2 lipofection reagent and MCF10A cells with Dharmafect1. For both methods, stable shRNA and transient siRNA, knockdown of CHFR expression was confirmed using semiquantitative duplex reverse transcription-PCR (RT-PCR) and Western blotting followed by densitometry.

Western blotting. To assess CHFR protein levels in asynchronous cells, 60.0 μ g of total protein from 70% to 80% confluent cell cultures were separated on 10% SDS-PAGE gels using the Criterion or Ready gel systems (Bio-Rad Laboratories) and immunoblotted to Hybond-P polyvinylidene



difluoride membrane (Amersham Biosciences). Following 1 h of incubation in a blocking solution of 2.5% nonfat dry milk and 0.1% TBS-Tween 20, a monoclonal antibody (mAb) against CHFR (Abnova) was used at a 1:500 dilution in 2.5% nonfat dry milk and 0.05% TBS-Tween 20 and incubated overnight at 4°C. CHFR was detected by hybridization with a goat anti-mouse/horseradish peroxidase (HRP) secondary antibody (Cell Signaling Technology) at a 1:2,000 dilution in 2.5% nonfat dry milk and 0.05% TBS-Tween 20. For a loading control, blots were blocked in 5% nonfat dry milk and 0.1% TBS-Tween 20 for 1 h. The blots were then stripped and immunoblotted again with an antibody against glyceraldehyde-3-phosphate dehydrogenase (GAPDH) as a control. The anti-GAPDH antibody (Abcam) was used at a 1:10,000 dilution and detected with a goat anti-mouse/HRP secondary antibody at a 1:5,000 dilution, both in 5% nonfat dry milk and 0.05% TBS-Tween 20. The SuperSignal West Pico chemiluminescent kit (Pierce) was used for detection and blots were exposed to Kodak Biomax XAR film. Relative expression of CHFR was assessed by using the IS-1000 Digital Imaging System (Alpha Innotech Corp.) for densitometry to determine signal intensity, and then a ratio of CHFR/GAPDH was calculated. CHFR expression was considered low if the ratio of relative expression was <0.5, which was the lowest value among the IHMEC lines.

RT-PCR. For semiquantitative duplex RT-PCR, reaction conditions were optimized as described previously (28). Briefly, primer concentrations were optimized to create equal band intensity between *CHFR* and the internal *GAPDH* loading control, and the cycle number that resulted in the logarithmic phase of product generation was determined. Total RNA was isolated from BCCs and IHMECs via the Qiagen RNeasy RNA isolation kit. cDNA was then generated from 1.0 µg of total RNA using the Qiagen Omniscript Reverse Transcription kit (Qiagen, Inc.) and random hexamer primers. CHFR cDNA was amplified with the following primers (forward/reverse, 5'-3'): CAGCAGTCCAGGATTACGTGTG/AGCAGTCAG-GACGGGATGTTAC (500 bp) or TCCCCAGCAATAAACTGGTC/GTATGC-CAGTTGTGTTCG (205 bp). GAPDH cDNA was amplified with the following primers (forward/reverse, 5'-3'): AGTCCATGCCATCACTGCCA/GGTGTCGCTGTTGAAGTCAG (340 bp). PCR products were separated on a 1.0% agarose gel in 1× Tris-borate EDTA and stained with ethidium bromide. Band intensity was assessed using the IS-1000 Digital Imaging System.

For quantitative RT-PCR, cDNA samples from IHMECs and BCC lines were amplified in triplicate from the same total RNA sample following the manufacturer's instructions. Samples were amplified using Taqman MGB FAM dye-labeled in an ABI7900HT model Real-time PCR machine (Applied Biosystems). To amplify *CHFR* cDNA, probe set Hs00217191_m1 was used, whereas the control, *GAPDH*, was amplified with probe set Hs99999905_m1 (Applied Biosystems).

Tissue samples and immunohistochemistry. The monoclonal anti-CHFR antibody was used at a 1:50 dilution for hybridization to paraffin-embedded sections of human breast tissue using standard methods. Primary antibody was detected following protocols described by the manufacturer (DakoCytomation), using diaminobenzidine as a chromogen and with Harris hematoxylin counterstain (Surgipath Medical Industries). Optimization and validation of the immunostaining conditions was done on multi-organ TMAs using a DAKO autostainer.

To study CHFR expression in primary breast cancers, 160 paraffin-embedded patient samples arrayed on a single high-density TMA were used for the analysis (29). Details on this TMA have been described previously (30). Tissue cores from 98 patients with invasive breast carcinoma were available to evaluate CHFR staining. The staining was scored using a four tiered scoring system (1, negative; 2, weak; 3, moderate; and 4, strong) by two independent trained investigators in the Department of Pathology (C.G.K. and L.D.) and ChromaVision computerized scoring (Clariant, Inc.). The Wilcoxon rank test was used to determine if there was an association between CHFR staining and clinicopathologic variables, including patient age, tumor size, tumor grade, lymph node status, estrogen receptor (ER), progesterone receptor (PR), HER2/*neu* status, and patient survival. To determine CHFR staining in normal mammary epithelia, paraffin-embedded tissues from patients were prepared as above. Digital images were obtained with an Olympus BX-51 microscope and SPOT camera system at either a ×40 or ×60 objective magnification.

Growth curve analysis. To determine the growth rate of the cellular population, 4×10^4 cells were plated into each well in six-well plates. Cells from three different wells were then manually counted with a hemacytometer. A new set of three wells were counted every 2 to 3 days for a total of 7 or 9 days, at which point at least one cell line began to reach confluence. Average cell numbers from the three wells were then plotted as a function of a time.

Immunofluorescence and mitotic index. Early mitotic chromosomes were identified via immunofluorescence using a phospho-histone H3-Ser28 antibody (Upstate) at a 1:100 dilution and anti-rabbit Alexa Fluor 488 secondary antibody at a 1:500 dilution both diluted in blocking solution. Cells were blocked in 5% nonfat dry milk, 1% bovine serum albumin (BSA), and 0.025% Triton X-100 solution in PBS for 1 h before incubation with primary antibody. Cells were counterstained with phalloidin conjugated to Alexa Fluor 568 to detect the actin cytoskeleton and ProLong Gold antifade reagent with 4',6-diamidino-2-phenylindole (DAPI) to detect all nuclei (both available from Molecular Probes/Invitrogen). Cells were visualized using a compound Leica DMRB microscope with a Leitz laser at ×63 magnification (W. Nuhsbaum, Inc.). The mitotic index was calculated as the number of H3-Ser28-stained nuclei from 1,000 total (DAPI stained) nuclei and then converted to a percentage.

To assess for vimentin staining, cells were plated 24 h before staining at a density of 3×10^4 cells per chamber in two-chambered slides. MCF10A cells that were transiently transfected with a pool of four *CHFR* siRNAs were transfected 48 h before seeding for immunofluorescence. Cells were blocked in 5% nonfat dry milk, 1% BSA, and 0.025% Triton X-100 solution in PBS for 1 h before incubation with primary antibody. Staining was done using an anti-vimentin antibody (1:40; Sigma-Aldrich), which was hybridized in blocking buffer overnight at 4°C, and detected with an anti-mouse/Alexa Fluor 594 secondary antibody in blocking buffer for 1 h at room temperature. Cells were counterstained with phalloidin/Alexa Fluor 488 and preserved in ProLong Gold antifade mounting media with DAPI. Cells were visualized using a compound Leica DMRB microscope with a Leitz laser at ×63 magnification and an Optronics camera system.

Apoptosis assay/Annexin V detection. Cells were seeded at 3×10^5 cells per well in six-well plates and transiently transfected with *CHFR* siRNA

Figure 2. A decrease in CHFR expression in IHMECs causes increased population growth rates, a higher number of cells entering metaphase (mitotic index), and an impaired checkpoint response to nocodazole. *A, top*, Western blotting shows a dramatic loss of CHFR protein following stable shRNA expression by retroviral transduction and transient siRNA transfection. HPV4-12 with CHFR shRNA 3 had at least a 60% decrease, whereas MCF10A with CHFR shRNA 123 showed nearly an 80% stable knockdown of CHFR expression compared with parental and scrambled shRNA controls. Transient siRNA transfection resulted in a 95% decrease in HPV4-12 cells and an ~99% decrease in MCF10A cells of CHFR protein. *Bottom*, semiquantitative duplex RT-PCR indicates a corresponding decrease in *CHFR* mRNA levels by ~70% for each cell line compared with controls. *B*, growth curves for HPV4-12 cells (*left*) and MCF10A cells (*right*) following stable shRNA expression (▲) compared with the parental cell lines (◆) and the scrambled shRNA (■) negative control cell lines. Cells were counted in triplicate every 2 days until at least one line reached confluency. *Points*, average number of cells counted on each day per cell line. Cells with decreased CHFR expression by shRNA had a faster growth rate compared with the parental and scrambled shRNA controls. *C*, the mitotic index of cells with or without CHFR shRNA is represented as the average percentage of histone H3-Ser28-stained nuclei, which is a marker of early metaphase cells, of $\geq 1,000$ total (DAPI stained) nuclei from triplicate experiments for each cell line. Cells were either untreated (*left*) or treated with 0.67 µmol/L nocodazole (*right*) to test for checkpoint response. Cells with decreased CHFR expression by shRNA showed approximately a 6-fold increase in mitotic cells without treatment and a 4- or 10-fold increase in mitotic cells after nocodazole treatment when compared with the parental and scrambled shRNA controls. *D*, transiently decreasing CHFR by siRNA in MCF10A cells, but not HPV4-12 cells, results in an increase in apoptosis in response to nocodazole. An Annexin V antibody was used to detect the presence of Annexin V on the cell surface. Cells were counterstained with propidium iodide and assessed by flow cytometry. Percentage of Annexin V-positive and propidium iodide-negative (apoptotic) cells. *, $P \leq 0.05$; **, $P \leq 0.001$, as determined by ANOVA.

or the siControl negative control as described previously. Fifty-two hours after transfection, cells were treated with either 0.67 $\mu\text{mol/L}$ nocodazole or 1.0 $\mu\text{mol/L}$ paclitaxel for 20 h. Cells were then collected and labeled for Annexin V on the cell surface and DNA was stained with propidium iodide using the Vybrant Apoptosis Assay kit 2 according to the manufacturer's instructions (Molecular Probes/Invitrogen). Cells were then analyzed by flow cytometry and the apoptotic cells were those that stained for Annexin V on the cell surface but were negative for propidium iodide staining. The graphs presented indicate the percentage of apoptotic cells as assessed by flow cytometry.

Matrigel invasion assay. This invasion assay was done according to the manufacturer's instructions (BD Biosciences). In short, 2.5×10^4 cells suspended in media without chemoattractant were plated in triplicate in Matrigel baskets in a 24-well plate. In the chamber below the baskets, either media without chemoattractant as a negative control or media with chemoattractant were added. Chemoattractants for each cell line are the following: (a) HPV4-12 cells: 5% fetal bovine serum (FBS), 1.0 $\mu\text{g/mL}$ hydrocortisone, 10.0 $\mu\text{g/mL}$ insulin, 100.0 ng/mL cholera toxin, and 10.0 ng/mL epidermal growth factor (EGF); (b) MCF10A cells: 10% horse serum, 0.5 $\mu\text{g/mL}$ hydrocortisone, 100.0 ng/mL cholera toxin, 10.0 $\mu\text{g/mL}$ insulin, and 20.0 ng/mL EGF; and (c) Hs578T cells: 10% FBS and 10.0 $\mu\text{g/mL}$ insulin.

Cells were incubated for 22 h at 37°C in 5% CO_2 for MCF10A and Hs578T cells or 10% CO_2 for HPV4-12 cells. The interior of the chambers was cleaned and the cells on the exterior were fixed and stained using the PROTOCOL Hema 3 staining kit (Fisher Scientific Co.). The number of stained cells that had traveled through the Matrigel collagen matrix was counted using a Nikon TMS inverted microscope at $\times 10$ magnification.

Scrape motility assay. Cells were grown to confluency in six-well plates and the cell monolayer was mechanically scarred using a plastic pipette tip. Cells were visualized for movement into the scratched surface with a Leica DMIRB inverted microscope with phase-contrast optics and a $10\times$ objective lens. Images were captured with a SPOT camera system (Diagnostic Instruments, Inc., Sterling Heights, MI). The motility phenotype was quantified by using the ImageQuant version 5.2 software package (GE Healthcare/Amersham Biosciences) to determine the area of the initial scrape and then the area of the same wound 24 h later. Data are presented as the percentage of the scraped area that remains after the end point.

Cellular morphology. Cellular morphology was recorded when cultured cells reached 100% confluence. Images were gathered using a Leica DMIL inverted microscope (W. Nuhsbaum) at $\times 10$ magnification and a SPOT RT Color camera with SPOT Advanced digital imaging software (Diagnostic Instruments).

Soft agar assay for colony formation. To do the soft agar assay, an underlayer of a 1:1 mixture of 1.2% noble agar and cell line appropriate growth media with 40% serum was added to six-well plates and allowed to solidify at room temperature for ~ 15 min. To create the overlayer for each well, we combined 2.0 mL growth media with 40% serum, 1.0 mL of 1.2% noble agar, 0.6 mL water, and 1.0×10^4 cells and added it on top of the solidified underlayer. The solution solidified at room temperature for 15 min. Cells were maintained at 37°C in a humidified incubator with the appropriate levels of CO_2 and two to three drops of media were added to each well every 3 days. After 30 days, the number of colonies present in the overlayer was counted manually.

Ploidy status and nucleolar changes. Cells were collected at 70% confluence by trypsinization and resuspended in 0.075 mol/L KCl on ice for 30 min. Cells were fixed in a 3:1 mixture of methanol and glacial acetic acid with mild vortexing, dropped onto glass slides, and stained with 544 $\mu\text{g/mL}$ Giemsa solution. To determine ploidy, the number of chromosomes was counted in at least 25 metaphases for each cell line and its derivatives.

To assess nucleolar changes, cells were prepared as described above and the number of nucleoli was counted in at least 50 cells, in triplicate, for each cell line. For both methods listed here, images were recorded with a compound Leitz DMRB microscope at $\times 40$ magnification and an Optronics camera.

Statistical analysis. The ANOVA test was used to determine statistical significance when comparing quantitative phenotypic differences between

parental, negative control, and CHFR-altered cells. The Wilcoxon signed-rank test and the Student's *t* test were done to assess statistical significance when analyzing patient data from the TMA. Student's *t* test was used to confirm a lack of statistical significance between parental and negative control cells for each experiment. For all tests, statistical significance was defined as $P \leq 0.05$. Error bars in the graphs presented here represent the SE.

Results

CHFR expression in BCC lines. We initially did Western blotting to assess CHFR expression in BCC and IHMEC lines. We noted variable expression among the BCC lines. Densitometry analysis revealed that 41% (9 of 22) of asynchronous BCC lines seemed to have low or no CHFR expression compared with the lowest amount of expression observed among four IHMEC cell lines, whereas only one cell line, MDA-MB-157, had expression higher than the range observed in IHMEC cells (Fig. 1A). The remaining lines had expression levels that fell within the range of IHMEC cells.

Previous reports indicated that *CHFR* mRNA was low in 50% of BCC lines as assessed by Northern blot analysis (31). In this study, quantitative RT-PCR was used to better define the levels of *CHFR* mRNA from asynchronous BCC lines compared with IHMECs. mRNA was collected from cells at 70% to 80% confluency, the same confluency used for Northern blot analysis. Quantitative RT-PCR revealed that only 17% of BCCs show *CHFR* expression levels significantly lower than IHMECs (data not shown). The difference between Northern blot analysis and quantitative RT-PCR may be due to the much higher sensitivity of quantitative RT-PCR to low amounts of sample or perhaps some transcripts were more easily detected by the quantitative RT-PCR probe compared with the probe used for Northern blotting. The lack of a direct correlation between mRNA levels by quantitative RT-PCR and protein expression suggests that CHFR protein expression may be altered by post-transcriptional or post-translational modification.

CHFR expression in primary breast cancers. As expected, CHFR staining by immunohistochemistry was prominent in the mammary gland epithelia from normal primary breast tissue (Fig. 1B). We next wanted to determine if CHFR expression was altered in primary breast cancers and if expression correlated with clinical and pathologic patient variables. From 160 patient samples of invasive breast carcinoma present on the TMA, 142 were available to score for CHFR staining and 98 had complete clinicopathologic data for statistical analysis. Of the 142 patient samples of invasive breast cancer scored for CHFR staining, 36% were negative, but only 0.5% showed strong CHFR staining. The numbers of patient samples per staining score are as follows: negative (1), 51; weak (2), 35; moderate (3), 48; and strong (4), 8 (Fig. 1C). Patient samples were annotated for several clinicopathologic variables, including tumor size, ER status, PR status, HER2/*neu* expression, lymph node status, patient age, and tumor grade. Primary samples were classified as positive for CHFR staining and expression if they scored between two and four in staining intensity. Because there is no published evidence as to a threshold of expression that is required for proper CHFR function, we included all positively stained samples in our analysis. Interestingly, there was a trend toward positive CHFR staining being correlated with ER-positive tumors ($P = 0.0903$, Wilcoxon rank test; $P = 0.0653$, *t* test; Fig. 1D). There was a striking significant correlation between positive CHFR staining and small (< 2 cm) tumor size ($P = 0.0179$, Wilcoxon rank test).

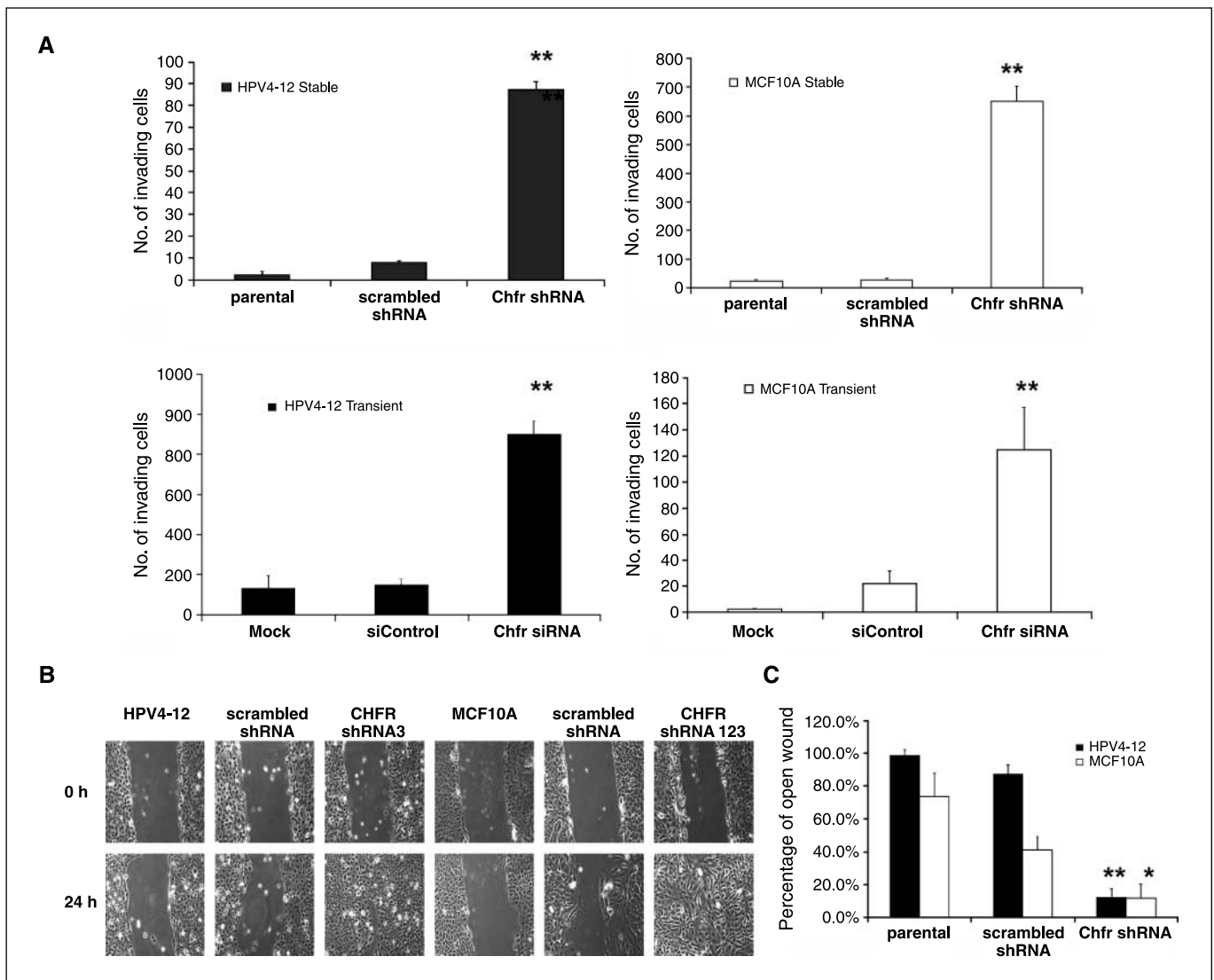


Figure 3. Decreasing CHFR expression using shRNA and siRNA in IHMECs leads to dramatic increases in invasive potential and motility. *A*, both stable (*top*) and transient (*bottom*) knockdown of CHFR expression results in greatly increased invasive potential through a Matrigel collagen matrix for both HPV4-12 cells (*left*) and MCF10A cells (*right*) compared with the control cell lines (parental/mock-transfected and scrambled shRNA/siControl). *Top left*, HPV4-12 with stable CHFR shRNA; *top right*, MCF10A with stable CHFR shRNA; *bottom left*, HPV4-12 with transient CHFR siRNA; *bottom right*, MCF10A with transient CHFR siRNA. *B*, digital phase-contrast images at $\times 10$ magnification showing an increase in motility (closing a scraped wound in confluent culture) for HPV-12 (*far left*) and MCF10A (*middle*) cells following stable CHFR shRNA expression compared with controls. *Top*, the initial wound in the culture; *bottom*, wound closure after 24 h (MCF10A) or 48 h (HPV4-12). *C*, graphical representation of the degree of wound closure depicted above. Motility is described as the percentage of the original wounded area that remains vacant after incubation. The area of the vacant surface was calculated using ImageQuant version 5.2 software. **, $P \leq 0.001$, ANOVA testing.

Stable loss of CHFR results in increased growth rates and impairs the checkpoint. CHFR expression was significantly decreased using a stably expressed shRNA construct, as determined by Western blotting and semiquantitative duplex RT-PCR, in two IHMEC lines, HPV4-12 and MCF10A (Fig. 2*A*). Stable expression of shRNA reduced the amount of CHFR protein by at least 60% in HPV4-12 cells and by $\sim 80\%$ in MCF10A cells and reduced the amount of mRNA by $\sim 70\%$ as determined by densitometry.

We first noticed that when CHFR expression was decreased by shRNA, the population growth rate dramatically increased for both IHMECs by at least 3-fold over the course of 7 to 9 days (MCF10A, $P \leq 0.03$; HPV4-12, $P \leq 0.001$; Fig. 2*B*). To understand this increase in population growth, we assessed the percentage of mitotic cells by using immunofluorescence to stain cells for the mitotic marker

phospho-histone H3-Ser28, a residue that is phosphorylated during metaphase and is gradually dephosphorylated in anaphase and is associated with the initiation of chromosome condensation (32). CHFR has been shown to delay chromosome condensation as part of the checkpoint response (2). Therefore, phospho-H3-Ser28 as a marker of condensed chromosomes is a good method to determine if the cells have passed through the CHFR checkpoint and entered the later stages of mitosis. This method was also used to determine mitotic index, which was calculated as the percentage of phospho-H3-Ser28-positive cells in the population. There was a statistically significant, 5- to 6-fold increase in the number of H3-Ser28-stained (mitotic) cells in the population when CHFR expression was lowered by shRNA in both cell lines. This showed that more cells went through the CHFR checkpoint, entering the later stages of

mitosis, with or without the stress of microtubule poisons, such as nocodazole ($P < 0.05$; Fig. 2C). In addition, the increase in phospho-H3-Ser28-positive cells following nocodazole treatment indicated that the checkpoint response to microtubule stress was bypassed when CHFR expression was decreased by shRNA (Fig. 2C, right). A similar increase in H3-Ser28 phosphorylation was observed when HPV4-12 cells were transiently transfected with a pool of four siRNAs for 72 h before staining to decrease CHFR protein by ~95% (Fig. 2A; data not shown).

To determine if significantly decreasing CHFR expression would alter the apoptotic response of the cells, we tested untreated or nocodazole-treated cells for the presence of Annexin V on the cell surface by flow cytometry and used propidium iodide staining to differentiate between apoptotic and necrotic cells (33). We found no difference between the cell lines with and without CHFR when they were untreated, which suggested that the increase in growth rates observed in the cells was not due to a decrease in cell death. In addition, there was no statistically significant difference in HPV4-12 cells transiently transfected with *CHFR* siRNA when compared with the mock- and siControl-transfected cells following treatment with nocodazole. However, when CHFR expression was transiently decreased in MCF10A cells, there was a 3-fold increase in apoptotic cells following nocodazole treatment ($P < 0.05$; Fig. 2D).

The stable loss of CHFR leads to enhanced invasive potential and increased motility. To determine if decreasing CHFR expression would cause phenotypic changes reminiscent of cellular transformation, IHMECs with or without *CHFR* shRNA were

subjected to the Matrigel invasion assay and the scrape (wound) motility assay. Surprisingly, there was a dramatic increase in the ability of the cells to invade through the Matrigel collagen matrix when CHFR expression was low: a 23-fold increase for MCF10A cells and a 5-fold increase for HPV4-12 cells ($P \leq 0.001$ for both; Fig. 3A). This dramatic change was also observed after transient transfection with a pool of four siRNAs, each targeting a different locus in *CHFR*, which indicated that this phenotype is directly caused by CHFR loss and is not a result of clonal selection during culture of the stable shRNA lines (Fig. 2A; Fig. 3A, bottom).

To assess changes in cellular motility, a wound was created in a confluent culture of IHMEC cells with or without *CHFR* shRNA. Motility was described as the percentage of the area of the initial wound that remained after a recovery period. IHMEC lines are not readily motile when their growth surface has been damaged and the remnants of the initial wound are clearly visible days later. However, when CHFR expression was decreased by stable shRNA, the cells became so motile that the wound was nearly entirely closed after 24 h (Fig. 3B and C). This was not a function of the increased population growth rates as cells with filopodia were clearly seen in the center of the wound <24 h later. In addition, the assay was completed before the population doubling time as indicated in the growth curves presented in Fig. 2B.

Stably decreased levels of CHFR causes morphologic changes and induces colony formation in soft agar. Normally, cells contain only one or two nucleoli in a nucleus and one frequently characterized change in cancer cells is increased number

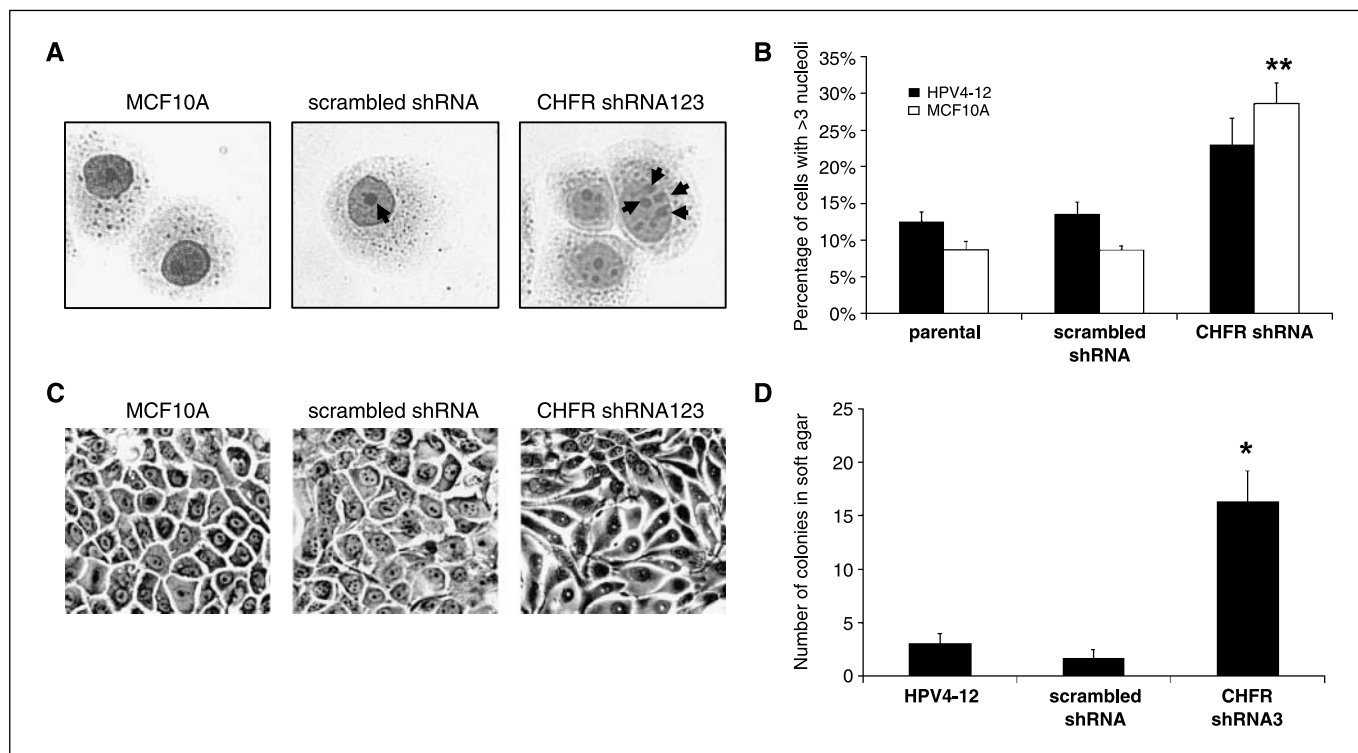


Figure 4. Decreasing CHFR expression causes nucleolar and morphologic changes and results in increased colony formation in soft agar. *A*, Giemsa-stained cells in which the nucleolus is depicted as a dark spot within the nucleus. Parental (far left) and scramble shRNA controls (middle) normally contain one or two nucleoli, whereas CHFR shRNA cells more frequently had greater than three nucleoli (arrows). *B*, graphical representation of the percentage of cells with greater than three nucleoli for each cell line ($n = 50$ for each of three trials). *C*, MCF10A cells visualized by phase-contrast light microscopy show a change in cellular shape from epithelial to an elongated morphology reminiscent of an epithelial-to-mesenchymal transition when CHFR expression is decreased by shRNA expression. *D*, 3-fold increase in colonies formed by HPV4-12 cells when CHFR expression is decreased. Ten thousand cells were suspended in a mixture of noble agar and complete growth media and allowed to grow for 30 d. *, $P < 0.05$; **, $P \leq 0.001$, as calculated with the ANOVA test for significance.

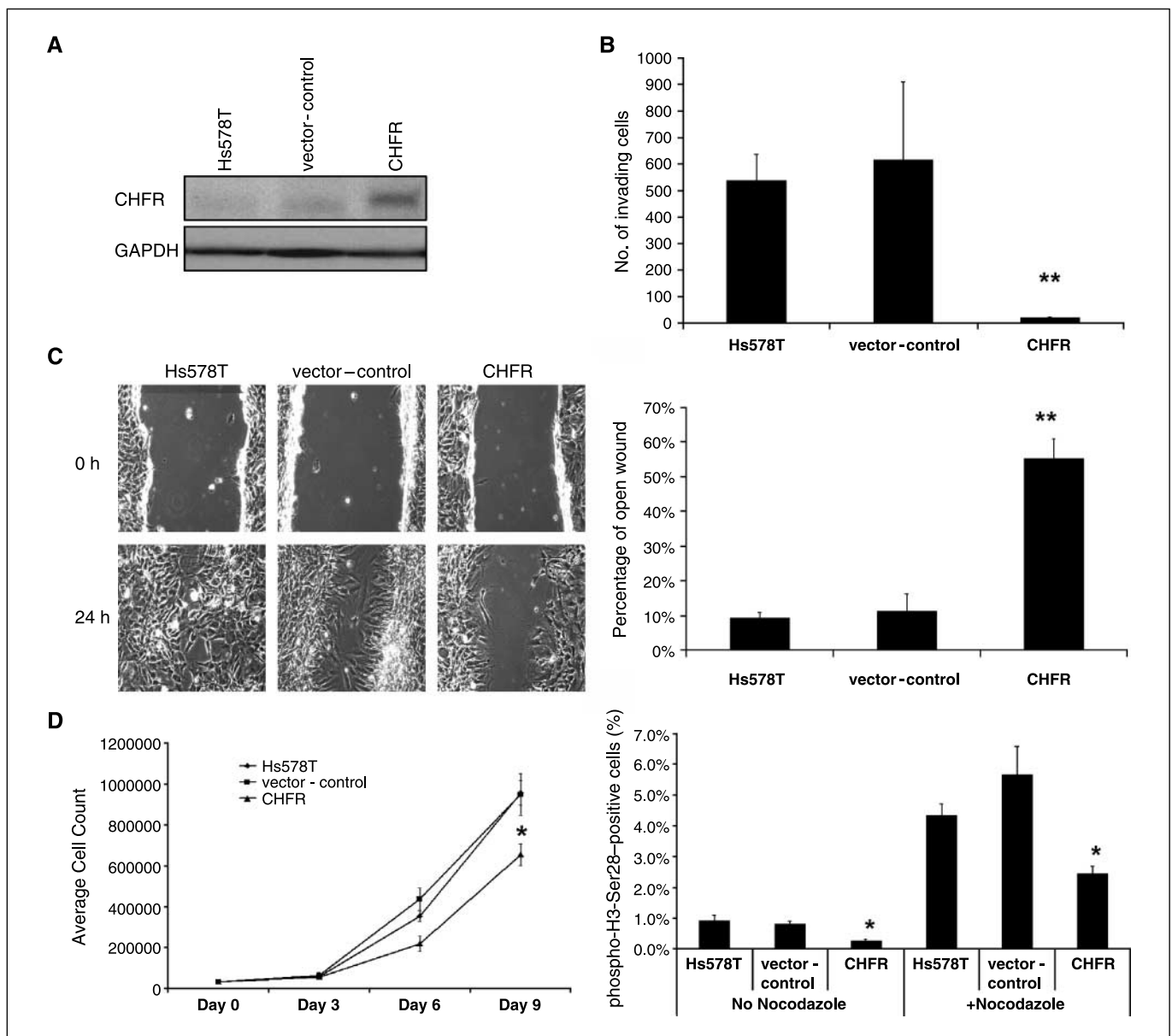


Figure 5. Stably increasing CHFR by retroviral transduction of a full-length *CHFR* cDNA construct in a BCC line, Hs578T, rescues some malignant phenotypes. *A*, Western blot showing increased CHFR expression (top) in cells retrovirally transduced with a Flag-tagged CHFR construct. GAPDH is used as a loading control (bottom). *B*, overexpression of CHFR in Hs578T cancer cells results in 25-fold loss of invasive potential through a Matrigel collagen matrix. *C*, left, phase-contrast images at $\times 10$ magnification showing a decrease in motility for Hs578T cells following stable CHFR overexpression. Top, initial wound in the culture; bottom, wound closure after 24 h. Hs578T cells overexpressing CHFR were less motile than their control counterparts and could not sufficiently close the wound in <24 h. Right, graphical representation of the degree of wound closure depicted on the (left). Percentage of the original scraped area remaining after incubation for each cell line. *D*, left, growth curve analysis over the span of 9 d showed that Hs578T BCCs overexpressing CHFR (\blacktriangle) had a slower growth rate, as indicated by a lower average cell count, than the parental (\blacklozenge) or the vector negative control (\blacksquare), despite being seeded at equal densities on day 0. Right, immunofluorescence staining for phospho-histone H3-Ser28 was used as a marker for mitotic cells. The percentage of cells positive for phospho-H3-Ser28 staining of at least 1,000 total nuclei (DAPI stained) is presented for each cell line. Overexpression of CHFR led to $\sim 50\%$ less mitotic cells compared with parental and empty vector controls in both untreated and nocodazole (200 ng/mL and 0.67 μ M/L) treated cells, indicating at least a partially restored checkpoint and a decrease in proliferation in untreated cells. *, $P < 0.05$; **, $P \leq 0.001$, calculated by ANOVA.

or more prominent nucleoli. In fact, changes in the number of nucleoli (more than three) are strongly correlated with a negative prognosis for survival in breast cancer patients (34). Interestingly, both IHMEC cell lines exhibited a marked increase in the number of nucleoli present in the nucleus, which was defined as three or more nucleoli, when CHFR expression was knocked down by shRNA. We found that 29% of MCF10A/CHFR shRNA cells (compared with 9% for controls; $P \leq 0.001$) and 23% of HPV4-12/CHFR shRNA cells had

greater than three nucleoli (compared with 13% for controls; $P \leq 0.08$; Fig. 4A and B). This change in nucleolar organization and number may indicate alterations in cellular metabolism related to proliferation, genome organization, or gene expression.

Further evidence for the acquisition of tumorigenic phenotypes following knockdown of CHFR expression was noticed only in MCF10A cells. We observed that MCF10A cells with CHFR shRNA underwent a morphologic change following ~ 10 passages in

culture. These immortalized mammary epithelial cells became elongated and showed more variability in cell size, which is suggestive of the epithelial-to-mesenchymal transition that is often observed during tumorigenesis (Fig. 4B). Further confirmation of this transition was indicated by increased expression of vimentin, a marker of mesenchymal cells, as shown by immunofluorescence (Supplementary Fig. S1).

To determine if the loss of CHFR altered the tumorigenicity of these cell lines, parental, scrambled shRNA, and CHFR shRNA-expressing cells were suspended in a mix of soft agar and growth media and assessed for their ability to form colonies. The MCF10A cell line has already been characterized as being tumorigenic in soft agar and the loss of CHFR did not enhance this phenotype. However, the HPV4-12 cell line does not form colonies in soft agar but when CHFR expression was decreased by shRNA, there was a modest but very significant increase in the number of colonies formed in soft agar ($P < 0.001$; Fig. 4D), indicating that these cells potentially had become tumorigenic.

Overexpression of CHFR reverses tumorigenic phenotypes in BCCs. In the converse experiment from above, we next determined if CHFR overexpression would have any affect on a tumorigenic BCC line, Hs578T, which has no endogenous expression of CHFR protein. Hs578T cells overexpressed *CHFR* through a stably transduced retroviral construct containing the full-length cDNA (Fig. 5A). Ectopically expressing CHFR in these BCCs did not alter their apoptotic response to nocodazole and it did not decrease colony formation in soft agar (data not shown). However, CHFR overexpression rescued other tumorigenic phenotypes in this cell line, making the cells act less like cancer cells. Importantly, we observed a dramatic change in invasiveness and motility. When Hs578T cells had higher CHFR levels, their ability to invade through a Matrigel collagen matrix plummeted by 25-fold ($P \leq 0.001$; Fig. 5B). Hs578T cells overexpressing CHFR showed nearly a 6-fold decrease in motility using the scrape assay ($P \leq 0.001$; Fig. 5C, right). In addition, overexpression of CHFR resulted in a statistically significant decrease in growth rates ($P < 0.05$; Fig. 5D, left) and a decrease in mitotic cells, as indicated by positive phospho-histone H3-Ser28 staining by immunofluorescence as described above ($P < 0.05$; Fig. 5D, right).

Stable knockdown of CHFR expression leads to genomic instability. Because genomic instability, or aneuploidy, was reported previously for mouse embryonic fibroblasts derived from the *Chfr* knockout mouse (11), we assessed the ploidy status of IHMECs shortly after stable *CHFR* shRNA expression. Strikingly, 60% to 70% of the cells with low CHFR were aneuploid, as opposed to <5% of cells in the normally hyperdiploid (48–49 chromosomes) parental lines (Fig. 6A and B). For aneuploid cells, the number of chromosomes present ranged from 49 to >85. Aneuploidy was also confirmed by fluorescence-activated cell sorting analysis as an increase in the population of cells with greater than 4N DNA content (data not shown).

Discussion

The findings presented here contribute significantly to the characterization of *CHFR* as a tumor suppressor gene. We show that CHFR protein expression was lost in many BCC lines and primary cancers, with nearly identical percentages (41% versus 36%). In addition, we provide evidence that decreasing CHFR mRNA and protein using shRNA/siRNA resulted in two IHMEC cell lines acquiring phenotypes associated with malignant

progression. These phenotypes included increased growth rates and mitotic indexes, the cells acquired the abilities of invasion and motility, and a striking percentage of cells became aneuploid. In addition, the HPV4-12 cells without CHFR were able to form colonies in soft agar, an indication of cellular transformation, and the MCF10A cells without CHFR became sensitive to microtubule poisons and underwent an epithelial-to-mesenchymal morphology change. When CHFR was overexpressed in Hs578T BCCs, the data suggested that higher CHFR levels did not have any adverse consequences in this cancer cell line and, in fact, reversed some tumorigenic phenotypes, thereby further supporting the role of CHFR as a tumor suppressor. When the CHFR expression data are combined with the results of the phenotypic analysis *in vitro* and the correlation with tumor size *in vivo*, it seems that the loss of CHFR is relevant to tumorigenesis in mammary epithelial cells.

In regards to primary invasive breast carcinoma, the correlation between CHFR staining and small tumor size, a very important prognostic indicator, is remarkable and supports a role for CHFR as a tumor suppressor. This is consistent with observations *in vitro*, in which decreased CHFR expression led to a dramatic increase in population growth rates and a higher percentage of mitotic cells. In addition, the putative association of CHFR and ER expression may provide continued support of a role for CHFR as a biomarker for breast cancer treatment. This is particularly relevant given previous clinical trials that showed ER-positive, and therefore

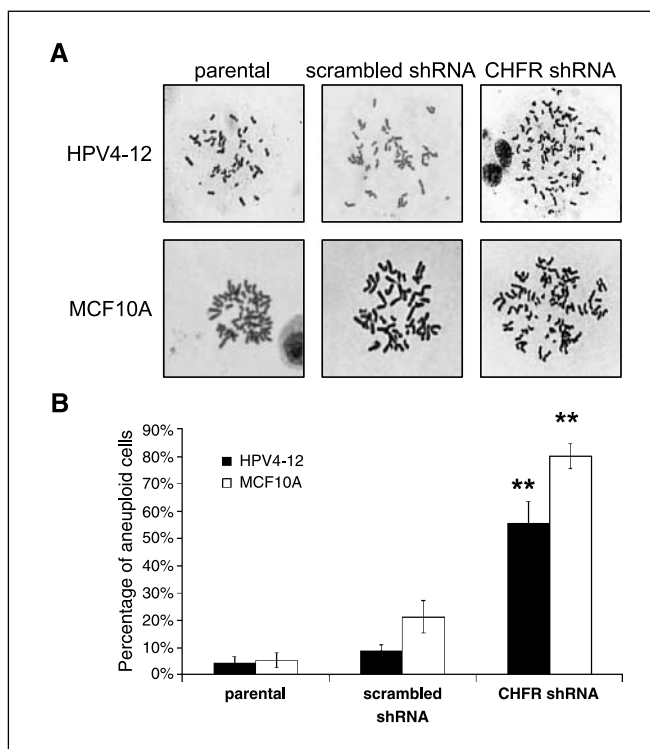


Figure 6. Decreased CHFR expression causes genomic instability. A, Giemsa-stained metaphase spreads of parental, negative control, and CHFR shRNA cells. IHMECs with lowered CHFR expression showed a greatly increased incidence of aneuploidy (>48 or 49 chromosomes). Both IHMEC cell lines are hyperdiploid and normally have either 48 chromosomes (MCF10A) or 49 chromosomes (HPV4-12). B, quantification of aneuploidy in CHFR shRNA cells showing that low CHFR expression results in 55% to 72% of the cells in the population becoming aneuploid. Percentage of aneuploid cells, from 25 counted metaphases per trial, for each cell line. **, $P \leq 0.001$, as determined by the ANOVA test for significance.

possibly CHFR-positive, breast cancers did not respond as well to paclitaxel treatment as ER-negative breast cancers (35–37). This corresponds well with previously published work describing CHFR-negative cells as sensitive to microtubule poisons in culture, undergoing apoptosis sooner than their CHFR-positive counterparts. This correlation between CHFR expression and apoptotic response to microtubule poisons was also observed in this work in the MCF10A cell line, which further substantiates a role for CHFR as a biomarker for drug response. In addition, the weak association of expression between ER and CHFR may help to elucidate another molecular pathway, in which CHFR functions to mediate cell proliferation or a common means of gene expression regulation.

Importantly, decreased CHFR expression led to an increase in the number of mitotic (metaphase and anaphase) cells in the population. Previously, this phenotype had only been described to occur in the presence of nocodazole and was thought to be due to an impaired checkpoint. However, the fact that this phenomenon also occurs without microtubule poisons suggests that CHFR can possibly play a wider role in regulating the timing of mitotic entry. This may help explain why the growth rates were faster in cells stably expressing *CHFR* shRNA and why tumors from breast cancer patients are larger when CHFR staining is absent.

Two of the most striking changes that resulted from altering CHFR expression were changes in invasion and motility of cells *in vitro*. This is the first time that CHFR has been implicated in a functional role other than cell cycle regulation. Considering its proposed role of monitoring microtubule dynamics as indicated by its initiation of the checkpoint in response to microtubule stress, it is hypothesized that CHFR has an even larger part in cytoskeletal organization, in which loss would more easily allow for the necessary reorganization of the cytoskeletal network required for motility. In addition, if the phenotypes observed in culture are found to mirror those seen in cancer patients (i.e., patients with low CHFR tumors have a higher incidence of distant metastases), then CHFR expression may be an indicator for tumor stage and/or patient prognosis.

Our report that low CHFR expression leads to genomic instability corroborates previously published work in the mouse (11). These data are suggestive of a problem with the structure or function of the mitotic spindle that is not corrected due to an impaired CHFR checkpoint. However, it could also indicate a defect in cytokinesis, which is plausible because work with the two yeast orthologues of CHFR show an interaction with the septin cytoskeletal network and they function in both the spindle checkpoint and cytokinesis (38, 39). Given the relatively frequent occurrence of low/lost CHFR in many types of tumors, this work may begin to explain the conundrum of the prevalence of aneuploidy in cancers but the lack of defective spindle checkpoint mediators, such as the MAD and BUB proteins.

It is not surprising that the same phenotypes were not always observed in the two cell lines tested. This is likely due to the unique genetic defects that caused the immortalization of the cell lines, thereby providing a clue to the genetic and physical interactions that CHFR has within the cell. Specifically, the HPV4-12 cell line was immortalized with the HPV E6/E7 protein to inhibit p53 and pRb function, whereas the MCF10A line was spontaneously immortalized following a t(3;9)(p14;p21) translocation that disrupted the *p15/p16* gene in addition to other chromosomal rearrangements (40, 41). The genetic differences may help to explain why MCF10A cells undergo a morphologic change and an increase in apoptosis in response to microtubule poisons after *CHFR* shRNA, whereas HPV4-12 cells do not. Differences may also be attributed to the fact that these two IHMEC lines are grown in different media with different levels of CO₂, but it should be noted that the media are very similar and contain nearly identical supplements.

This work on the phenotypic changes that arise *in vitro* with CHFR expression variation provides a unique insight as to what may happen in cancer patients and presents many new avenues through which to study CHFR expression, function, and molecular interactions. We report for the first time a correlation between CHFR levels and clinicopathologic variables in primary breast cancer, tumor size and perhaps ER status. We also comprehensively characterize the phenotypic changes that resemble cellular transformation in normal IHMEC cells when CHFR expression is substantially reduced. Through the combined findings of this work, we find the loss of CHFR to be an interesting dichotomy in breast cancer. This report shows that, on one hand, the loss of CHFR expression may indicate a larger and more aggressive tumor, whereas, in a surprising beneficial twist, it also makes the cancer cells sensitive to traditional chemotherapeutic agents that target the microtubules. It seems that as evidence builds, CHFR is gaining more time in the spotlight as a novel tumor suppressor as it aspires to be the next biomarker in cancer characterization.

Acknowledgments

Received 11/7/2006; revised 3/4/2007; accepted 4/5/2007.

Grant support: Department of Defense Breast Cancer Research Predoctoral Fellowship #BC050310 and NIH National Research Service Award #5-T32-GM07544 from the National Institute of General Medicine Sciences (L.M. Privette); NIH National Cancer Institute (NCI) grant RO1CA072877 (E.M. Petty); and NIH NCI grants K08CA090876 and RO1CA107469 and Department of Defense grant DAMD17-01-1-490 (C.G. Kleer).

The costs of publication of this article were defrayed in part by the payment of page charges. This article must therefore be hereby marked *advertisement* in accordance with 18 U.S.C. Section 1734 solely to indicate this fact.

We thank Esther Peterson for helpful suggestions and discussion; Nancy McAnsh and Donita Sanders for technical assistance with immunohistochemistry protocols; Thomas Giordano, M.D., for primary normal breast tissue samples; and Stephen Ethier, Ph.D., for the HPV and SUM breast cell lines.

References

1. Scolnick DM, Halazonetis TD. Chfr defines a mitotic stress checkpoint that delays entry into metaphase. *Nature* 2000;406:430–5.
2. Summers MK, Bothos J, Halazonetis TD. The CHFR mitotic checkpoint protein delays cell cycle progression by excluding cyclin B1 from the nucleus. *Oncogene* 2005; 24:2589–98.
3. Dang C, Hudis C. Adjuvant taxanes in the treatment of breast cancer: no longer at the tip of the iceberg. *Clin Breast Cancer* 2006;7:51–8.
4. Sakai M, Hibi K, Kanazumi N, et al. Aberrant methylation of the CHFR gene in advanced hepatocellular carcinoma. *Hepatogastroenterology* 2005;52:1854–7.
5. Satoh A, Toyota M, Itoh F, et al. Epigenetic inactivation of CHFR and sensitivity to microtubule inhibitors in gastric cancer. *Cancer Res* 2003;63:8606–13.
6. Chaturvedi P, Sudakin V, Bobiak ML, et al. Chfr regulates a mitotic stress pathway through its RING-finger domain with ubiquitin ligase activity. *Cancer Res* 2002;62:1797–801.
7. Ogi K, Toyota M, Mita H, et al. Small interfering RNA-induced CHFR silencing sensitizes oral squamous cell cancer cells to microtubule inhibitors. *Cancer Biol Ther* 2005;4:773–80.
8. Kang D, Chen J, Wong J, Fang G. The checkpoint protein Chfr is a ligase that ubiquitinates Plk1 and inhibits Cdc2 at the G₂ to M transition. *J Cell Biol* 2002;156:249–59.
9. Matsusaka T, Pines J. Chfr acts with the p38 stress kinases to block entry to mitosis in mammalian cells. *J Cell Biol* 2004;166:507–16.
10. Shivelman E. Promotion of mitosis by activated protein kinase B after DNA damage involves polo-like kinase 1 and checkpoint protein CHFR. *Mol Cancer Res* 2003;1:959–69.
11. Yu X, Minter-Dykhouse K, Malureanu L, et al. Chfr is required for tumor suppression and Aurora A regulation. *Nat Genet* 2005;37:401–6.

12. Brandes JC, van Engeland M, Wouters KA, Weijnenberg MP, Herman JG. CHFR promoter hypermethylation in colon cancer correlates with the microsatellite instability phenotype. *Carcinogenesis* 2005;26:1152-6.
13. Cheung HW, Ching YP, Nicholls JM, et al. Epigenetic inactivation of CHFR in nasopharyngeal carcinoma through promoter methylation. *Mol Carcinog* 2005;43:237-45.
14. Corn PG, Summers MK, Fogt F, et al. Frequent hypermethylation of the 5' CpG island of the mitotic stress checkpoint gene Chfr in colorectal and non-small cell lung cancer. *Carcinogenesis* 2003;24:47-51.
15. Honda T, Tamura G, Waki T, Kawata S, Nishizuka S, Motoyama T. Promoter hypermethylation of the Chfr gene in neoplastic and non-neoplastic gastric epithelia. *Br J Cancer* 2004;90:2013-6.
16. Mariatos G, Bothos J, Zacharatos P, et al. Inactivating mutations targeting the chfr mitotic checkpoint gene in human lung cancer. *Cancer Res* 2003;63:7185-9.
17. Mizuno K, Osada H, Konishi H, et al. Aberrant hypermethylation of the CHFR prophase checkpoint gene in human lung cancers. *Oncogene* 2002;21:2328-33.
18. Shibata Y, Haruki N, Kuwabara Y, et al. Chfr expression is downregulated by CpG island hypermethylation in esophageal cancer. *Carcinogenesis* 2002;23:1695-9.
19. Tokunaga E, Oki E, Nishida K, et al. Aberrant hypermethylation of the promoter region of the CHFR gene is rare in primary breast cancer. *Breast Cancer Res Treat* 2006;97:199-203.
20. Toyota M, Sasaki Y, Satoh A, et al. Epigenetic inactivation of CHFR in human tumors. *Proc Natl Acad Sci U S A* 2003;100:7818-23.
21. Andrieux J, Demory JL, Morel P, et al. Frequency of structural abnormalities of the long arm of chromosome 12 in myelofibrosis with myeloid metaplasia. *Cancer Genet Cytogenet* 2002;137:68-71.
22. Aubele M, Auer G, Braselmann H, et al. Chromosomal imbalances are associated with metastasis-free survival in breast cancer patients. *Anal Cell Pathol* 2002;24:77-87.
23. Dohna M, Reincke M, Mincheva A, Allolio B, Solinas-Toldo S, Lichter P. Adrenocortical carcinoma is characterized by a high frequency of chromosomal gains and high-level amplifications. *Genes Chromosomes Cancer* 2000;28:145-52.
24. Heidenblad M, Schoenmakers EF, Jonson T, et al. Genome-wide array-based comparative genomic hybridization reveals multiple amplification targets and novel homozygous deletions in pancreatic carcinoma cell lines. *Cancer Res* 2004;64:3052-9.
25. Rutherford S, Hampton GM, Frierson HF, Moskaluk CA. Mapping of candidate tumor suppressor genes on chromosome 12 in adenoid cystic carcinoma. *Lab Invest* 2005;85:1076-85.
26. Ethier SP, Mahacek ML, Gullick WJ, Frank TS, Weber BL. Differential isolation of normal luminal mammary epithelial cells and breast cancer cells from primary and metastatic sites using selective media. *Cancer Res* 1993;53:627-35.
27. Neve RM, Chin K, Fridlyand J, et al. A collection of breast cancer cell lines for the study of functionally distinct cancer subtypes. *Cancer Cell* 2006;10:515-27.
28. Erson AE, Niell BL, DeMers SK, Rouillard JM, Hanash SM, Petty EM. Overexpressed genes/ESTs and characterization of distinct amplicons on 17q23 in breast cancer cells. *Neoplasia* 2001;3:521-6.
29. Van den Eynden GG, Van der Auwera I, Van Laere S, et al. Validation of a tissue microarray to study differential protein expression in inflammatory and non-inflammatory breast cancer. *Breast Cancer Res Treat* 2004;85:13-22.
30. Kleer CG, Cao Q, Varambally S, et al. EZH2 is a marker of aggressive breast cancer and promotes neoplastic transformation of breast epithelial cells. *Proc Natl Acad Sci U S A* 2003;100:11606-11.
31. Erson AE, Petty EM. CHFR-associated early G₂/M checkpoint defects in breast cancer cells. *Mol Carcinog* 2004;39:26-33.
32. Goto H, Tomono Y, Ajiro K, et al. Identification of a novel phosphorylation site on histone H3 coupled with mitotic chromosome condensation. *J Biol Chem* 1999;274:25543-9.
33. Vermes I, Haanen C, Steffens-Nakken H, Reutelingsperger C. A novel assay for apoptosis. Flow cytometric detection of phosphatidylserine expression on early apoptotic cells using fluorescein labelled Annexin V. *J Immunol Methods* 1995;184:39-51.
34. van Diest PJ, Mouriquand J, Schipper NW, Baak JP. Prognostic value of nucleolar morphometric variables in cytological breast cancer specimens. *J Clin Pathol* 1990;43:157-9.
35. Berry DA, Cirincione C, Henderson IC, et al. Estrogen-receptor status and outcomes of modern chemotherapy for patients with node-positive breast cancer. *JAMA* 2006;295:1658-67.
36. Poole C. Adjuvant chemotherapy for early-stage breast cancer: the tAnGo trial. *Oncology (Huntingt)* 2004;18:23-6.
37. Sezgin C, Karabulut B, Uslu R, et al. Potential predictive factors for response to weekly paclitaxel treatment in patients with metastatic breast cancer. *J Chemother* 2005;17:96-103.
38. Fraschini R, Bilotta D, Lucchini G, Piatti S. Functional characterization of Dma1 and Dma2, the budding yeast homologues of *Schizosaccharomyces pombe* Dma1 and human Chfr. *Mol Biol Cell* 2004;15:3796-810.
39. Guertin DA, Venkatram S, Gould KL, McCollum D. Dma1 prevents mitotic exit and cytokinesis by inhibiting the septation initiation network (SIN). *Dev Cell* 2002;3:779-90.
40. Band V, Zajchowski D, Kulesa V, Sager R. Human papilloma virus DNAs immortalize normal human mammary epithelial cells and reduce their growth factor requirements. *Proc Natl Acad Sci U S A* 1990;87:463-7.
41. Cowell JK, LaDuca J, Rossi MR, Burkhardt T, Nowak NJ, Matsui S. Molecular characterization of the t(3;9) associated with immortalization in the MCF10A cell line. *Cancer Genet Cytogenet* 2005;163:23-9.

Loss of CHFR in Human Mammary Epithelial Cells Causes Genomic Instability

Lisa M. Privette¹, Jingly Fung Weier², Ha Nam Nguyen³, and Elizabeth M. Petty^{1,4}

¹*Department of Human Genetics, University of Michigan, Ann Arbor, MI 48109,*

²*Department of Ob/Gyn and Reproductive Sciences, University of California, San*

Francisco, San Francisco, CA 94143, ³ Institute for Stem Cell Biology and Regenerative

Medicine, Stanford University, Palo Alto, CA 94304, and ⁴ Department of Internal

Medicine, University of Michigan, Ann Arbor, MI 48109

Corresponding Author:

Elizabeth M. Petty

5220A MSRBIII
1150 W. Medical Center Drive
Ann Arbor, MI, 48109-0638

epetty@umich.edu
fax: 734-647-7979
phone: 734-763-2532

Key words: aneuploidy, tubulin, cell cycle checkpoints, mitosis, mitotic spindle

Running title: Loss of CHFR leads to genomic instability

Abbreviations:

CHFR: Checkpoint with FHA and RING Finger

HDI: Histone Deacetylase Inhibitor

IHMECs: Immortalized Human Mammary Epithelial Cells

SKY: Spectral Karyotyping

Abstract:

CHFR is an E3 ubiquitin ligase and early mitotic checkpoint protein implicated in many cancers, including breast cancer. To investigate the potential role of CHFR in maintaining genomic stability prior to breast cancer development, we decreased CHFR expression by siRNA in MCF10A cells and visualized chromosome segregation by immunofluorescence. Knockdown of CHFR expression in genomically stable MCF10A cells resulted in aneuploidy caused by mitotic defects including misaligned metaphase chromosomes, lagging anaphase chromosomes, multi-polar poorly formed mitotic spindles, and multi-nucleated cells. CHFR siRNA also increased Aurora A expression and caused MAD2 and BUBR1 mislocalization during mitosis, suggesting that CHFR may be involved in the mitotic spindle checkpoint and genomic instability. Furthermore, we found that CHFR interacted with both Aurora A and MAD2. These findings, along with CHFR's reported role in responding to microtubule poisons, suggested that CHFR might also interact with tubulins. We discovered that CHFR interacted with, and ubiquitinated, α -tubulin and CHFR siRNA increased expression of both unmodified and acetylated α -tubulin. Importantly, our results suggest a novel role for CHFR regulating chromosome segregation where decreased expression, as seen in cancer cells, contributes to genomic instability.

Introduction:

Checkpoint with FHA and RING Finger (CHFR) is recognized as a novel mitotic stress checkpoint pathway regulator and biomarker for treatment response to taxanes. It delays cells in prophase, prior to the mitotic spindle checkpoint, after microtubule poison exposure (i.e. nocodazole or paclitaxel) [1-7]. Subsequently, CHFR has been implicated in oncogenesis. *CHFR* expression is lost or decreased in tumors compared to normal tissues, sometimes due to promoter hypermethylation [5, 7-13]. Importantly, CHFR is a strong tumor suppressor in both a knockout mouse model [14] and in immortalized human mammary epithelial cells (IHMECs) and breast cancer cell lines [3]. Long-term loss of CHFR expression led to abnormal chromosome complements (i.e. aneuploidy) in both models.

Aneuploidy is a hallmark of many cancers and may result from diverse mitotic defects including multi-polar spindles secondary to aberrant cytokinesis or centrosome amplification, sister chromatid cohesion defects, incorrect centromere attachment, or an impaired mitotic spindle assembly checkpoint (“spindle checkpoint”) [15]. The spindle checkpoint prevents chromosome mis-segregation during cell division by delaying anaphase until the kinetochores of all sister chromatids are attached to the microtubules of the mitotic spindle. Spindle checkpoint gene mutations are rare, especially in breast cancers, but many cancer cells have an impaired or unregulated spindle checkpoint [15-17].

Aurora A kinase is crucial for centrosome amplification and maturation, mitotic entry, and spindle assembly [18-20]. Aurora A over-expression can override the spindle checkpoint, resulting in mitotic defects and mislocalization of the key spindle checkpoint

proteins BUBR1 and MAD2, among others [21, 22]. Aurora A is amplified and/or overexpressed in many cancers and correlates with improved patient survival following treatment with microtubule-targeting taxanes [23, 24]. Importantly, Aurora A may be a target for CHFR-mediated ubiquitination and subsequent proteasome degradation [14]. This suggests that CHFR expression may be important for genome stability and cellular responses to taxanes potentially through its regulation of Aurora A expression.

We hypothesized that the transient loss of CHFR causes genomic instability due to defects in mitotic spindle formation and function, potentially through Aurora A overexpression. To test this, we transiently decreased CHFR expression by siRNA in the genomically stable IHMEC cell line, MCF10A. Subsequent analysis of these cells using revealed they were aneuploid, had four major mitotic defects as visualized by immunofluorescence, showed mislocalization of the key spindle checkpoint proteins BUBR1 and MAD2, and had increased expression of mitotic proteins including Aurora A, α -tubulin, and acetylated α -tubulin.

Materials and Methods:

Cell Culture

MCF10A and HEK293 cells were obtained from the American Type Culture Collection and cultured under recommended conditions. For CHFR knockdown, cells were untransfected (“mock”) or transfected with 2.0 μ M of either a non-targeting siControl siRNA or siRNAs targeting CHFR using Dharmafect1 according to manufacturer’s instructions and analyzed 72 hours later (siGENOME, Dharmacon RNA Technologies). Cells were transfected with 6.0 μ g of a Flag-tagged Aurora A construct (gift of Xiaochun Yu, University of Michigan) or Flag-tagged CHFR using FuGENE 6 (Roche) and lysates were harvested 24 hours later. Cells were treated with 15 μ M of MG132 (Calbiochem) for ten hours and/or 200 ng/ml of nocodazole (Sigma) for 18 hours. To induce DNA damage, cells were treated with 0.3 μ M aphidicolin for 24 hours.

SKY and Metaphase Spreads

MCF10A cells were treated with 50 ng/ml colcemid (Invitrogen) for 16 hours then collected and re-suspended in a hypotonic solution of 2% KCl and 2% $\text{Na}_3\text{C}_6\text{H}_5\text{O}_7$ for 7 minutes at 37°C. Metaphase spreads were then prepared and stained with Giemsa as previously described [3]. At least 25 metaphases were counted in triplicate for each sample.

SKY analysis was performed according to the manufacturer's protocol (Applied Spectral Imaging) and as previously described [25]. Briefly, cells and slides were prepared as described above and unstained slides were aged in 2x SSC, treated with pepsin (Amresco; 30 μ g/mL in 0.01 N HCl), then rinsed with PBS. Slides were post-fixed in 1% paraformaldehyde in PBS/MgCl₂ and dehydrated in an ethanol series before and

after denaturation in a 70% Formamide/2x SSC solution. The denatured SKY probes (Vial 1, SKY kit, Vista, CA) were hybridized to the slides and incubated at 37°C for two days. Following washings, antibodies (from vial 3 and 4, SKY kit) were added and incubated at 37°C for one hour each. The slides were counterstained with DAPI in anti-fade solution. All images were acquired using an SD200 SpectraCube spectral imaging system (ASI) attached to a Nikon E800 microscope consisting of an optical head (a Sagnac interferometer) coupled to a multi-line charge-coupled device camera (Hamamatsu, Bridgewater, NJ). Spectral Imaging (v. 2.6.1) and Sky View (v. 1.6.2) were used to acquire and analyze the images, respectively. The average of ten metaphases was used to create the consensus karyotype.

Western Blotting

Whole cell lysates were collected from approximately 80% confluent cultures. For samples analyzed for ubiquitination of α -tubulin, 2mM of N-ethylmaleimide (NEM; Sigma) was added to the lysis buffer. Western blots were prepared as previously described [3]. Western blot membranes were blocked for one hour at room temperature, and incubated overnight at 4°C in primary antibody. The following antibodies were used: a mouse CHFR mAb (1:500 dilution, Abnova Corp.), a custom rabbit polyclonal antibody to the N-terminus of CHFR (1:1000), and a rabbit anti-Aurora A antibody (1.0 mg/ml, gift of Xiaochun Yu). A mouse anti- α -tubulin, mouse anti- γ -tubulin, mouse anti-acetylated α -tubulin, rabbit anti-Flag (all Sigma-Aldrich), rabbit anti- α -tubulin (Cell Signaling Technology), and a rabbit anti-GST (Santa Cruz) were all used at a 1:1000 dilutions. Anti-ubiquitin (1:100, Sigma) was also used and an anti-glyceraldehyde-3-phosphate dehydrogenase antibody (1:10,000, Abcam) was used for a loading control.

Blots were incubated in secondary antibody, anti-mouse:HRP or anti-rabbit:HRP, diluted in the blocking solution (both from Cell Signaling Technology). We used the SuperSignal West Pico chemiluminescent kit (Pierce) and exposed the blots to Kodak Biomax XAR film. Blots were stripped prior to re-probing with a different antibody. Where applicable, blots were analyzed from three experiments to verify expression changes. Densitometry was performed using the FluorChem 8900 imaging system (Alpha Innotech Corp.).

GST pull-down

A GST-CHFR fusion construct was created using the pGEX2T vector (Amersham) and expressed in the DH5 α strain of *E. coli*. Logarithmic *E. coli* cultures were collected in lysis buffer (2.5 mM PMSF in 1.0% Triton X-100 with a protease inhibitor cocktail from Roche), sonicated, and then cleared by centrifugation. One milligram of *E. coli* lysates was combined with 50 μ l of washed Glutathione Sepharose 4B beads (Amersham) for two hours at 4°C. Then, one milligram of whole cell lysates from MCF10A cells were added to the beads and incubated overnight at 4°C. Following washes with NTEN200 buffer (20 mM Tris-HCl, 1 mM EDTA, 0.5% NP-40, 25 μ g/ml PMSF and 200 mM NaCl), the bound proteins were eluted with 10 mM glutathione and collected by centrifugation. Isolated proteins were identified by Western blotting.

Immunoprecipitation

Immunoprecipitations were completed according to manufacturer's instructions using the Protein G immunoprecipitation kit (Sigma). Briefly, whole cell lysates were combined with ten microliters of the specified antibody (mouse IgG₁ isotype control from BD BioSciences, mouse anti- α -tubulin, or mouse anti-Flag M2 antibody) and diluted in

the supplied 1x IP buffer and incubated for at least two hours at 4°C. Then, 50 microliters of protein G beads were added to the lysate/antibody mix overnight at 4°C. Following washes, the immunoprecipitated lysates were boiled in the columns in 40 microliters of 5x Laemmli's loading buffer then eluted by centrifugation and analyzed by Western blotting.

Immunofluorescence

MCF10A cells were plated in two-chambered slides then fixed in 4% paraformaldehyde and blocked in 5% milk, 1.0% BSA in 0.025% TBS-Triton X100. Staining was performed using an anti- α -tubulin antibody (1:100, Sigma), a rabbit anti-Aurora A antibody (1:50, Cell Signaling Technology) or an anti-Histone H3-phospho-Ser28 antibody (1:100, Upstate), all of which were hybridized in blocking buffer overnight at 4°C. Slides were hybridized with an anti-mouse:Alexafluor594 or an anti-rabbit:Alexafluor488 secondary antibody (Invitrogen Molecular Probes) diluted to 1:200 in blocking buffer. Samples were preserved with ProLong Gold anti-fade mounting media with DAPI (Invitrogen Molecular Probes).

For BUBR1 and MAD2 localization, cells were fixed in 4% paraformaldehyde then permeabilized for five minutes in 0.5% TritonX-100 dissolved in 1x PBS. Slides were blocked in 5% milk in 0.1% TBST then hybridized with an anti-BUBR1 antibody (Sigma Aldrich) or an anti-MAD2 antibody (BD BioSciences) at a 1:200 dilution in blocking buffer overnight at 4°C. Slides were hybridized with an anti-mouse:Alexafluor594 secondary antibody (1:500, Invitrogen) diluted in blocking buffer for 1h at room temperature then preserved with ProLong Gold anti-fade mounting media with DAPI (Invitrogen).

Microscopy

We used a compound Leica DMRB microscope (W. Nuhsbaum, Inc.) and either a 63x or a 100x objective lens. An external Leica EL6000 light source was used for immunofluorescence images. Images were recorded using a Retiga 2000R 12-bit digital camera and QCapture Pro v5.1 software (QImaging).

Data Analysis

Images were processed for resolution, magnification, and gamma settings using Adobe Photoshop CS2. We used the ANOVA test for statistical significance and $p < 0.05$ was considered significant. Error bars depict the standard error from triplicate experiments. One asterisk (*) indicates $p \leq 0.05$ and two asterisks (**) indicate $p \leq 0.001$.

Results:

Transient Loss of CHFR Expression Leads to Aneuploidy

We previously reported that the stable loss of CHFR expression by shRNA in IHMECs led to aneuploidy [3]. Further analysis by spectral karyotyping (SKY) revealed two distinct cell populations - minimally aneuploid or near tetraploid (Figure 1A compared to 1B and 1C). The karyotype of parental MCF10A cells was: 48,XX,1qhph,+del(1),der(3)t(3;9)(p14;p21),+del(7),i(8)(q10),der(9)t(3;9)(p14;p21)t(3;5). However, the consensus karyotype for the minimally aneuploid population was 47~50,XX,+X,t(1;2),der(3)t(3;9)(p14;p21),der(6)t(6;19),+del(7),der(9)t(3;9)(p14;p21)t(3;5),der(11)t(8;11), t(15;18),+20. The consensus karyotype for the near tetraploid population was 81-95,XXXX,-1,t(1;2),der(2)t(1;2),-3,der(3)t(3;9)(p14;p21)x2,-5,der(6)t(6;19)x2,+del(7),-9,der(9)t(3;9)(p14;p21)t(3;5),-10,der(11)t(8;11)x2,-13,der(15)t(15;18)x2,-17,-18x2,+20x2,-22. MCF10A cells with CHFR shRNA often gained chromosomes 20 and X and had four novel chromosomal translocations t(1;2), t(6;19), t(8;11), and t(15;18) (Figures 1B and 1C), suggesting that CHFR may regulate genomic stability via multiple mechanisms.

To determine if the genomic instability was a byproduct of prolonged culture following CHFR knockdown, MCF10A cells were transiently transfected with a pool of four siRNAs targeting CHFR ("MCF10:CHFR-siRNA cells") and analyzed for aneuploidy and chromosome breakage. CHFR expression was decreased by at least 80% after 72 hours as detected by Western blotting (Figure 1D). We observed no chromosome breaks on metaphase spreads following treatment with aphidicolin to induce DNA damage (data not shown). However, 32% of MCF10:CHFR-siRNA cells were

aneuploid, typically having 49-59 chromosomes, compared to the mock transfected and non-targeting (“siControl”) negative control counterparts 72 hours after transient transfection (Figures 1E and 1F, $p \leq 0.001$). This indicated that CHFR associated aneuploidy occurs quickly and is not simply a result of prolonged cell culture conditions. Given this, we wanted to elucidate the mechanism(s) by which aneuploidy occurred in IHMECs that had lost CHFR expression.

CHFR Regulates Chromosome Attachment to the Mitotic Spindle

We performed immunofluorescence to visualize chromosomes during mitosis to examine the cause of aneuploidy in MCF10A:CHFR-siRNA cells. Nearly 25% of MCF10A:CHFR-siRNA cells had metaphase chromosomes not properly located to the metaphase plate when compared to the control cells (Figures 2A and 2B), and lagging chromosomes and chromosome bridges during anaphase (Figure 2C). This suggested that the spindle checkpoint was disrupted in cells with decreased CHFR expression.

To test this hypothesis, we studied the localization of two critical spindle checkpoint proteins, BUBR1 and MAD2, during mitosis. Normally, both proteins have a punctate staining pattern early in mitosis, reflecting their localization to kinetochores. Staining becomes diffuse later in mitosis after all chromosomes are attached to the mitotic spindle. Normal BUBR1 and MAD2L1 staining patterns were observed in negative control cells (Figures 2D and 2E). In contrast, MCF10A:CHFR-siRNA cells demonstrated diffuse BUBR1 and MAD2 staining early in metaphase (Figures 2D and 2E, right panels). Although Western blotting showed that CHFR siRNA did not change MAD2 or BUBR1 expression, immunoprecipitation experiments revealed that CHFR could interact with MAD2, but not BUBR1 (Figure 2F, and data not shown).

One potential outcome of chromosome non-disjunction is the abortion of cytokinesis, resulting in bi-nucleated cells and potential tetraploidy [26]. As noted above, some cells with stably decreased CHFR by shRNA were tetraploid (Figure 1A). In fact, 6% of transiently transfected MCF10:CHFR-siRNA cells were binucleated, suggesting tetraploidy, compared to only about 1% of negative control cells (Figures 2G and 2H, $p < 0.05$). This was confirmed by the occasional tetraploid MCF10A:CHFR-siRNA metaphase spread when cells were assessed for aneuploidy.

CHFR Modulates Expression of Aurora A

The chromosome mis-segregation phenotypes in MCF10:CHFR-siRNA cells were highly reminiscent of mouse embryonic fibroblasts (MEFs) that over-express Aurora A [21]. Previous studies also performed in MEFs from CHFR knockout mice showed similar mitotic defects and Aurora A over-expression [14]. To assess this in our human mammary epithelial cell model, we performed Western blotting and found that MCF10A:CHFR-siRNA cells had much greater Aurora A expression compared to the control cells (Figure 3A). We also found that Flag-tagged Aurora A could interact with endogenous CHFR in MCF10A cells by immunoprecipitation (Figure 3B). The physical interaction of these two proteins, combined with Aurora A over-expression in MCF10:CHFR-siRNA cells, substantiates previously published observations that Aurora A is a target for CHFR-mediated ubiquitination for degradation [14].

Early in mitosis, Aurora A localizes to centrosomes where it mediates their maturation and separation and spindle formation [27]. We found that Aurora A localized to the centrosomes during metaphase in control cells, as evidenced by the two distinct dots that co-localized to the spindle poles. However, in 16% of MCF10:CHFR-siRNA

cells, more than two Aurora A foci were detected, indicating increased Aurora A expression and suggesting centrosome amplification (Figures 3C and 3D, $p < 0.05$).

CHFR Regulates α -tubulin Expression

In MCF10:CHFR-siRNA cells, the mitotic spindle was more condensed with poor polar microtubule formation (Figure 3C, bottom panel). Since CHFR is best known for its role in delaying mitotic entry due to stress on the microtubules, we hypothesized that CHFR may interact with, and possibly regulate, tubulin proteins. We performed a GST pull-down using a GST:CHFR fusion protein and lysates from MCF10A cells. We found that CHFR interacts with α -tubulin, but not β - or γ -tubulin, when the MCF10A cells were previously treated with nocodazole (Figure 4A and data not shown). In addition, this was confirmed by co-immunoprecipitation experiments, though the interaction was not dependent on nocodazole treatment using this method (Figure 4B).

To determine if CHFR can ubiquitinate α -tubulin, we treated MCF10A cells that had been transfected with control or CHFR siRNAs with the proteasome inhibitor MG132 with or without concomitant treatment with nocodazole. Following immunoprecipitation for α -tubulin and immunoblotting for ubiquitin, we found that CHFR is able to ubiquitinate α -tubulin during nocodazole exposure, as evidenced by the loss of ubiquitin signal in MCF10A:CHFR-siRNA cells (Figure 4C, lane 3 vs. lane 6). Western blotting confirmed that CHFR can regulate α -tubulin as there was a reproducible increase in α -tubulin protein levels, but not in β - or γ -tubulin, in MCF10A:CHFR-siRNA cells (Figure 4D and 4E and data not shown, $p < 0.05$). The amount of acetylated α -tubulin in MCF10A:CHFR-siRNA cells was consistently double that of controls (Figure 4C and 4D, $p < 0.05$).

Discussion:

The work presented here indicates that CHFR is extremely important for the maintenance of genomic stability in mammary epithelial cells. Our results support and help explain the findings of aneuploidy in MEFs from *Chfr* null mice and IHMEC lines. The observed chromosome rearrangements that we noted by spectral karyotyping likely resulted from prolonged culture and the disruption of DNA damage response genes secondary to the aneuploidy, which we have shown can develop within a few days after CHFR expression is decreased.. To the contrary, the presence of additional chromosomes with a numeric change in chromosome number, or aneuploidy, in cells treated with siRNA against *CHFR* provide powerful evidence that CHFR is required for genomic stability via proper chromosome segregation during mitosis. Furthermore, the lack of chromosome breaks on metaphase spreads from MCF10A cells transiently transfected with siRNA to decrease CHFR mRNA and protein suggested that CHFR might not participate directly in the DNA damage response induced by aphidicolin. This conclusion is supported by previous studies in which CHFR expression did not alter the DNA damage response following treatment with other genotoxic reagents [1, 28].

The mis-localization of the key checkpoint proteins, BUBR1 and MAD2, following CHFR knockdown indicated an impaired spindle checkpoint, which would help to explain the observed aneuploidy. With an impaired spindle checkpoint, cells with decreased CHFR expression could enter anaphase without all of their chromosomes localized to the metaphase plate, leading to the appearance of lagging chromosomes and unequal chromosome segregation amongst the two daughter cells. One potential outcome of improper chromosome segregation is the abortion of cytokinesis, resulting in bi-

nucleated cells and tetraploidy, which was also observed in this work [26]. Of interest, our work strongly agrees with previous findings that the yeast orthologs of CHFR, Dma1 and Dma2, also function in regulating the spindle checkpoint and cytokinesis [29, 30]. Further work, including live cell imaging, will help to clarify the mechanism(s) leading to lagging chromosomes.

It is quite interesting that CHFR can interact with one spindle checkpoint protein, MAD2, but not another, BUBR1. This suggests that CHFR interacts with MAD2 when it is not in the spindle checkpoint complex at the kinetochore. Despite CHFR's E3 ubiquitin ligase activity, MAD2 (and BUBR1) expression was not altered in CHFR knockdown cells, indicating that the protein-protein interaction between CHFR and MAD2 is not for the purposes of regulating MAD2 protein levels. However, it has been shown that CHFR has the potential to regulate lysine-63 based ubiquitin chains on target proteins, which would likely alter the target protein's activity or function rather than target it for degradation by the proteasome (Bothos). Further work is suggested in order to determine if CHFR can create Lys63-based ubiquitin chains or can mono-ubiquitinate MAD2 in order to alter its localization and/or function, and to examine if CHFR can interact with the open or closed conformations of MAD2, or both. Additional studies to determine if CHFR can interact with, or regulate, other mitotic spindle checkpoint proteins, such as Cdc20 or MAD1, will also be required to understand further the role of CHFR in the mitotic spindle checkpoint. It is apparent that the findings presented here concerning the role of CHFR in the spindle assembly checkpoint leave many unanswered questions, but they have also opened up many new potential avenues of future research.

We were able to confirm the previously published finding that CHFR can regulate Aurora A expression [14]. Aurora A is amplified and over-expressed in many cancers, including breast cancer, and over-expression in cultured cells leads to transformation [24, 27]. In addition, a transgenic mouse over-expressing Aurora A in the mammary epithelium leads to tumor formation and genomic instability [31]. CHFR was recently characterized as a tumor suppressor and, as shown here, many of its genomic instability phenotypes resemble Aurora A over-expression; therefore, we propose that one major mechanism by which CHFR inhibits oncogenesis may be through its negative regulation of Aurora A [3, 14]. Novel drugs currently are being generated that target the Aurora kinases [32]. Since decreased CHFR expression has been linked to sensitivity to microtubule-targeting drugs, future studies may find a synergistic effect when taxanes and Aurora kinase inhibitors are both used for treatment.

These findings also indicate that CHFR may play a role in regulating α -tubulin turnover or stability, especially following microtubule stress. This is the first clue as to how the “CHFR checkpoint” responds to microtubule poisons, though an unidentified signaling cascade also is likely to be involved in this checkpoint. The ubiquitination and possible degradation of α -tubulin may be necessary to remove those α/β tubulin dimers that are targeted by microtubule poisons. In unstressed cells, CHFR may also be required for proper spindle formation. Aurora A kinase is also required for proper spindle formation, supposedly through its positive regulation of a protein called HURP [33]. HURP is required for both chromosome congression and alignment and for the polymerization and stabilization of microtubules during mitotic spindle formation. Therefore, the capacity of CHFR to control spindle formation may be via its upstream

regulation of Aurora A, though it may also be due to CHFR's capability to ubiquitinate α -tubulin and control the amount of acetylated α -tubulin that is available for use during spindle assembly.

One of the effects of decreasing CHFR expression is the upregulation of the amount of acetylated α -tubulin protein. One of the characteristics of stabilized microtubules is the acetylation of α -tubulin on residue lysine 40. Acetylated α -tubulin is associated with decreased microtubule turnover and is localized to the mitotic spindle, centrosomes, and the mitotic midbody [34, 35]. An increase in acetylated α -tubulin, such as that observed here, would likely result in over-stabilized microtubules, which would hinder mitotic spindle movement or would prevent its proper formation. This may help to explain why CHFR negative cells are more sensitive to taxanes. The cellular stress of the excess of over-stabilized acetylated microtubules, combined with stress induced by microtubule poisons, may enable the cell to surpass a threshold of tolerable stress that would result in apoptosis. This hypothesis is supported by reports of a synergistic effect on both apoptotic response and microtubule stabilization, as indicated by acetylated α -tubulin, when endometrial cancer cells are treated with both the histone deacetylase inhibitor (HDI) trichostatin A and paclitaxel [36]. Interestingly, some of the targets of HDIs are also tubulin deacetylase proteins, such as HDAC6 and SIRT2 [37, 38]. Recent studies also show that treating cells with HDIs down-regulates Aurora A expression [39]. Future clinical studies may find that the synergistic effect between HDIs and taxanes may be different in CHFR-positive versus CHFR-negative cancer cells.

The finding that CHFR knockdown results in increased amounts of acetylated α -tubulin is particularly interesting because another protein that has been found to initiate a

“CHFR checkpoint-like” response to microtubule poisons is SIRT2, a tubulin and histone deacetylase [40]. SIRT2 over-expression is a phenocopy of CHFR over-expression in regards to the regulation of mitotic entry and response to mitotic stress. Therefore, hypothetically, decreased SIRT2 expression should resemble decreased CHFR expression in both response to mitotic stress and the amount of acetylated α -tubulin in the cell. Future studies should determine if the increase in acetylated α -tubulin after decreased CHFR expression is due to SIRT2 or through the activation of Aurora A-regulated HURP.

We also found that CHFR over-expression is toxic to many breast cell lines independent of the method of transfection or retroviral transduction (both transient and stable; data not shown). This suggests that CHFR expression must be tightly regulated – too much is toxic whereas too little causes genomic instability and tumorigenesis. This is reminiscent of other mitotic checkpoint proteins, such as MAD2, in that both too little and too much of the protein are deleterious [41]. Determining the mechanism(s) causing CHFR over-expression toxicity likely will answer many of the questions that remain about the function of CHFR.

These findings have led to us a propose model for how CHFR may regulate genomic instability and/or tumorigenesis (Figure 5). We suggest that decreased or lost CHFR expression causes over-expression of Aurora A and both unmodified and acetylated α -tubulin, and mis-localization of MAD2. Aurora A over-expression could lead to centrosome amplification, an impaired spindle checkpoint, and possibly defective mitotic spindle formation, leading to aneuploidy and impaired cytokinesis. The mis-localization of MAD2 also causes an impaired spindle checkpoint response. The increase

in acetylated α -tubulin could cause stress on the mitotic spindle. Both pathways would lead to genomic instability, contributing to tumorigenesis. As indicated by the generality of this model, much research remains in order to elucidate the role of CHFR in regulating mitosis and genomic instability. Cancer often develops in concert with the loss of cell cycle regulation and genomic instability; CHFR may function in both processes.

Acknowledgements:

This work was supported by a Department of Defense BCRP Fellowship, #BC050310, and by the NIH National Research Service Award #5-T32-GM07544 from the National Institute of General Medicine Sciences to LMP and an NIH NCI grant RO1CA072877 to EMP. We thank Esther Peterson for helpful suggestions, Xiaochun Yu for reagents and insightful discussions, and Sally Camper for sharing her Leica DMRB microscope.

References:

- [1] Chaturvedi, P, Sudakin, V, Bobiak, ML, Fisher, PW, Mattern, MR, Jablonski, SA, Hurle, MR, Zhu, Y, Yen, TJ, and Zhou, BB. Chfr regulates a mitotic stress pathway through its RING-finger domain with ubiquitin ligase activity. *Cancer Res.* 2002; 62: 1797-1801.
- [2] Ogi, K, Toyota, M, Mita, H, Satoh, A, Kashima, L, Sasaki, Y, Suzuki, H, Akino, K, Nishikawa, N, Noguchi, M, Shinomura, Y, Imai, K, Hiratsuka, H, and Tokino, T. Small interfering RNA-induced CHFR silencing sensitizes oral squamous cell cancer cells to microtubule inhibitors. *Cancer Biol Ther.* 2005; 4: 773-780.
- [3] Privette, LM, Gonzalez, ME, Ding, L, Kleer, CG, and Petty, EM. Altered expression of the early mitotic checkpoint protein, CHFR, in breast cancers: implications for tumor suppression. *Cancer Res.* 2007; 67: 6064-6074.
- [4] Sakai, M, Hibi, K, Kanazumi, N, Nomoto, S, Inoue, S, Takeda, S, and Nakao, A. Aberrant methylation of the CHFR gene in advanced hepatocellular carcinoma. *Hepatology.* 2005; 52: 1854-1857.
- [5] Satoh, A, Toyota, M, Itoh, F, Sasaki, Y, Suzuki, H, Ogi, K, Kikuchi, T, Mita, H, Yamashita, T, Kojima, T, Kusano, M, Fujita, M, Hosokawa, M, Endo, T, Tokino, T, and Imai, K. Epigenetic inactivation of CHFR and sensitivity to microtubule inhibitors in gastric cancer. *Cancer Res.* 2003; 63: 8606-8613.
- [6] Scolnick, DM, and Halazonetis, TD. Chfr defines a mitotic stress checkpoint that delays entry into metaphase. *Nature.* 2000; 406: 430-435.
- [7] Yanokura, M, Banno, K, Kawaguchi, M, Hirao, N, Hirasawa, A, Susumu, N, Tsukazaki, K, and Aoki, D. Relationship of aberrant DNA hypermethylation of CHFR with sensitivity to taxanes in endometrial cancer. *Oncol Rep.* 2007; 17: 41-48.
- [8] Corn, PG, Summers, MK, Fogt, F, Virmani, AK, Gazdar, AF, Halazonetis, TD, and El-Deiry, WS. Frequent hypermethylation of the 5' CpG island of the mitotic stress checkpoint gene Chfr in colorectal and non-small cell lung cancer. *Carcinogenesis.* 2003; 24: 47-51.
- [9] Erson, AE, and Petty, EM. CHFR-associated early G2/M checkpoint defects in breast cancer cells. *Mol Carcinog.* 2004; 39: 26-33.
- [10] Honda, T, Tamura, G, Waki, T, Kawata, S, Nishizuka, S, and Motoyama, T. Promoter hypermethylation of the Chfr gene in neoplastic and non-neoplastic gastric epithelia. *Br J Cancer.* 2004; 90: 2013-2016.
- [11] Mizuno, K, Osada, H, Konishi, H, Tatematsu, Y, Yatabe, Y, Mitsudomi, T, Fujii, Y, and Takahashi, T. Aberrant hypermethylation of the CHFR prophase checkpoint gene in human lung cancers. *Oncogene.* 2002; 21: 2328-2333.
- [12] Shibata, Y, Haruki, N, Kuwabara, Y, Ishiguro, H, Shinoda, N, Sato, A, Kimura, M, Koyama, H, Toyama, T, Nishiwaki, T, Kudo, J, Terashita, Y, Konishi, S, Sugiura, H, and Fujii, Y. Chfr expression is downregulated by CpG island hypermethylation in esophageal cancer. *Carcinogenesis.* 2002; 23: 1695-1699.
- [13] Toyota, M, Sasaki, Y, Satoh, A, Ogi, K, Kikuchi, T, Suzuki, H, Mita, H, Tanaka, N, Itoh, F, Issa, JP, Jair, KW, Schuebel, KE, Imai, K, and Tokino, T. Epigenetic

- inactivation of CHFR in human tumors. *Proc Natl Acad Sci U S A*. 2003; 100: 7818-7823.
- [14] Yu, X, Minter-Dykhouse, K, Malureanu, L, Zhao, WM, Zhang, D, Merkle, CJ, Ward, IM, Saya, H, Fang, G, van Deursen, J, and Chen, J. Chfr is required for tumor suppression and Aurora A regulation. *Nat Genet*. 2005; 37: 401-406.
 - [15] Kops, GJ, Weaver, BA, and Cleveland, DW. On the road to cancer: aneuploidy and the mitotic checkpoint. *Nat Rev Cancer*. 2005; 5: 773-785.
 - [16] Myrie, KA, Percy, MJ, Azim, JN, Neeley, CK, and Petty, EM. Mutation and expression analysis of human BUB1 and BUB1B in aneuploid breast cancer cell lines. *Cancer Lett*. 2000; 152: 193-199.
 - [17] Percy, MJ, Myrie, KA, Neeley, CK, Azim, JN, Ethier, SP, and Petty, EM. Expression and mutational analyses of the human MAD2L1 gene in breast cancer cells. *Genes Chromosomes Cancer*. 2000; 29: 356-362.
 - [18] Fu, J, Bian, M, Jiang, Q, and Zhang, C. Roles of Aurora kinases in mitosis and tumorigenesis. *Mol Cancer Res*. 2007; 5: 1-10.
 - [19] Mori, D, Yano, Y, Toyo-oka, K, Yoshida, N, Yamada, M, Muramatsu, M, Zhang, D, Saya, H, Toyoshima, YY, Kinoshita, K, Wynshaw-Boris, A, and Hirotsune, S. NDEL1 phosphorylation by Aurora-A kinase is essential for centrosomal maturation, separation, and TACC3 recruitment. *Mol Cell Biol*. 2007; 27: 352-367.
 - [20] Koffa, MD, Casanova, CM, Santarella, R, Kocher, T, Wilm, M, and Mattaj, IW. HURP is part of a Ran-dependent complex involved in spindle formation. *Curr Biol*. 2006; 16: 743-754.
 - [21] Anand, S, Penrhyn-Lowe, S, and Venkitaraman, AR. AURORA-A amplification overrides the mitotic spindle assembly checkpoint, inducing resistance to Taxol. *Cancer Cell*. 2003; 3: 51-62.
 - [22] Jiang, Y, Zhang, Y, Lees, E, and Seghezzi, W. AuroraA overexpression overrides the mitotic spindle checkpoint triggered by nocodazole, a microtubule destabilizer. *Oncogene*. 2003; 22: 8293-8301.
 - [23] Lassmann, S, Shen, Y, Jutting, U, Wiehle, P, Walch, A, Gitsch, G, Hasenburg, A, and Werner, M. Predictive value of Aurora-A/STK15 expression for late stage epithelial ovarian cancer patients treated by adjuvant chemotherapy. *Clin Cancer Res*. 2007; 13: 4083-4091.
 - [24] Zhou, H, Kuang, J, Zhong, L, Kuo, WL, Gray, JW, Sahin, A, Brinkley, BR, and Sen, S. Tumour amplified kinase STK15/BTAK induces centrosome amplification, aneuploidy and transformation. *Nat Genet*. 1998; 20: 189-193.
 - [25] McGhee, EM, Cotter, PD, Weier, JF, Berline, JW, Turner, MA, Gormley, M, and Palefsky, JM. Molecular cytogenetic characterization of human papillomavirus16-transformed foreskin keratinocyte cell line 16-MT. *Cancer Genet Cytogenet*. 2006; 168: 36-43.
 - [26] Shi, Q, and King, RW. Chromosome nondisjunction yields tetraploid rather than aneuploid cells in human cell lines. *Nature*. 2005; 437: 1038-1042.
 - [27] Marumoto, T, Zhang, D, and Saya, H. Aurora-A - a guardian of poles. *Nat Rev Cancer*. 2005; 5: 42-50.

- [28] Summers, MK, Bothos, J, and Halazonetis, TD. The CHFR mitotic checkpoint protein delays cell cycle progression by excluding Cyclin B1 from the nucleus. *Oncogene*. 2005; 24: 2589-2598.
- [29] Murone, M, and Simanis, V. The fission yeast *dma1* gene is a component of the spindle assembly checkpoint, required to prevent septum formation and premature exit from mitosis if spindle function is compromised. *Embo J*. 1996; 15: 6605-6616.
- [30] Guertin, DA, Venkatram, S, Gould, KL, and McCollum, D. Dma1 prevents mitotic exit and cytokinesis by inhibiting the septation initiation network (SIN). *Dev Cell*. 2002; 3: 779-790.
- [31] Wang, X, Zhou, YX, Qiao, W, Tominaga, Y, Ouchi, M, Ouchi, T, and Deng, CX. Overexpression of aurora kinase A in mouse mammary epithelium induces genetic instability preceding mammary tumor formation. *Oncogene*. 2006; 25: 7148-7158.
- [32] Manfredi, MG, Ecsedy, JA, Meetze, KA, Balani, SK, Burenkova, O, Chen, W, Galvin, KM, Hoar, KM, Huck, JJ, LeRoy, PJ, Ray, ET, Sells, TB, Stringer, B, Stroud, SG, Vos, TJ, Weatherhead, GS, Wysong, DR, Zhang, M, Bolen, JB, and Claiborne, CF. Antitumor activity of MLN8054, an orally active small-molecule inhibitor of Aurora A kinase. *Proc Natl Acad Sci U S A*. 2007; 104: 4106-4111.
- [33] Yu, CT, Hsu, JM, Lee, YC, Tsou, AP, Chou, CK, and Huang, CY. Phosphorylation and stabilization of HURP by Aurora-A: implication of HURP as a transforming target of Aurora-A. *Mol Cell Biol*. 2005; 25: 5789-5800.
- [34] Piperno, G, LeDizet, M, and Chang, XJ. Microtubules containing acetylated alpha-tubulin in mammalian cells in culture. *J Cell Biol*. 1987; 104: 289-302.
- [35] Webster, DR, and Borisy, GG. Microtubules are acetylated in domains that turn over slowly. *J Cell Sci*. 1989; 92 (Pt 1): 57-65.
- [36] Dowdy, SC, Jiang, S, Zhou, XC, Hou, X, Jin, F, Podratz, KC, and Jiang, SW. Histone deacetylase inhibitors and paclitaxel cause synergistic effects on apoptosis and microtubule stabilization in papillary serous endometrial cancer cells. *Mol Cancer Ther*. 2006; 5: 2767-2776.
- [37] North, BJ, Marshall, BL, Borra, MT, Denu, JM, and Verdin, E. The human Sir2 ortholog, SIRT2, is an NAD⁺-dependent tubulin deacetylase. *Mol Cell*. 2003; 11: 437-444.
- [38] Zhang, Y, Li, N, Caron, C, Matthias, G, Hess, D, Khochbin, S, and Matthias, P. HDAC-6 interacts with and deacetylates tubulin and microtubules in vivo. *Embo J*. 2003; 22: 1168-1179.
- [39] Park, JH, Jong, HS, Kim, SG, Jung, Y, Lee, KW, Lee, JH, Kim, DK, Bang, YJ, and Kim, TY. Inhibitors of histone deacetylases induce tumor-selective cytotoxicity through modulating Aurora-A kinase. *J Mol Med*. 2007;
- [40] Inoue, T, Hiratsuka, M, Osaki, M, Yamada, H, Kishimoto, I, Yamaguchi, S, Nakano, S, Katoh, M, Ito, H, and Oshimura, M. SIRT2, a tubulin deacetylase, acts to block the entry to chromosome condensation in response to mitotic stress. *Oncogene*. 2007; 26: 945-957.
- [41] Perez de Castro, I, de Carcer, G, and Malumbres, M. A census of mitotic cancer genes: new insights into tumor cell biology and cancer therapy. *Carcinogenesis*. 2007; 28: 899-912.

Figure Legends:

Figure 1: Decreased CHFR expression causes aneuploidy.

(A) SKY analysis of parental MCF10A cells shows the characteristic karyotype of this genomically stable hyper-diploid cell line. (B and C) SKY analysis of MCF10A cells stably expressing shRNA against CHFR are either minimally aneuploid (B) or nearly tetraploid (C) and show novel chromosome translocations. (D) Western blotting shows >80% decrease in CHFR expression in MCF10A cells transiently transfected with siRNA against CHFR (“CHFR siRNA”) compared to untransfected (“mock”) and non-targeting siRNA (“siControl”) transfected cells after 72 hours. (E) Metaphase spreads show that MCF10A:CHFR-siRNA cells (right panel) are aneuploid. Bar = 25 μ m. (F) The graph shows the frequency of aneuploidy in transiently transfected MCF10A cells.

Figure 2: Decreased CHFR expression impairs the mitotic spindle checkpoint.

(A) Chromosomes did not properly migrate to the metaphase plate in MCF10A:CHFR siRNA cells (arrow, right panel). Immunofluorescence (IF) detected phosphorylated Histone H3-Ser28 (green) to identify metaphase chromosomes. (B) A graph of the data shown in (A); 24% of cells with CHFR siRNA have chromosomes improperly located during metaphase. (C) MCF10A:CHFR-siRNA cells have lagging chromosomes and chromosome bridges during anaphase (arrow, right panel). DNA was stained blue with DAPI. Bar = 5 μ m. (D and E) IF to visualize BUBR1 and MAD2 reveals that cells with CHFR siRNA (right panels) have diffuse BUBR1 and MAD2 staining patterns (red, D and E respectively) indicating mislocalization. Control cells have the characteristic punctate staining patterns for BUBR1 and MAD2. DNA was stained blue with DAPI.

Bar = 5 μ m. (F) Endogenous MAD2 interacts with CHFR. HEK293 cells were transfected with a Flag-tagged CHFR construct, with or without nocodozaole treatment. Immunoprecipitation (IP) with an anti-Flag antibody was performed to isolate CHFR and subsequently analyzed by Western blotting (WB) for the Flag:CHFR fusion protein and endogenous MAD2. “Input” indicates 5% of the lysates used for the IP reaction. (G) Immunofluorescence to detect cytoskeletal α -tubulin (red) during interphase shows that MCF10A:CHFR-siRNA cells become binucleated (subpanels i and l; arrow) compared to the negative control cells (subpanels c and f). Bar = 50 μ m. (H) Quantification of the data shown in (F), in which 6% of MCF10A cells transfected with CHFR siRNA are binucleated compared to less than 2% of control cells. One asterisk (*) indicates that $p < 0.05$ while two asterisks (**) indicates that $p < 0.001$.

Figure 3: CHFR interacts with Aurora A and regulates its protein expression.

(A) MCF10A:CHFR-siRNA cells over-express Aurora A, as shown by Western blotting, compared to control cells. (B) Flag:Aurora A interacts with endogenous CHFR by co-immunoprecipitation. Lysates from MCF10A cells transiently transfected with Flag-tagged Aurora A were subjected to immunoprecipitation with an anti-Flag (M2) antibody then probed for CHFR or Flag by Western blotting using rabbit antibodies. “Input” on the left indicates 10% of the lysates used for the IP reaction. (C) Immunofluorescence for Aurora A (green) indicates that MCF10:CHFR-siRNA cells (bottom row) have greater than two Aurora A foci when compared to two foci in negative control cells during metaphase. Cells were stained with DAPI (blue) for DNA and for α -tubulin (red) to see the spindle. Note the compacted, disorganized mitotic spindle (red) in CHFR-siRNA

cells (subpanel l compared to subpanels d and h). (D) Quantification of the data in (C), showing that nearly 16% of MCF10A cells transfected with CHFR siRNA had greater than two Aurora A foci.

Figure 4: CHFR ubiquitinates α -tubulin and regulates α -tubulin protein expression.

(A) A GST pull-down using a GST:CHFR fusion protein shows that CHFR can interact with α -tubulin, but not β - or γ -tubulin from MCF10A whole cell lysates as shown by Western blotting for tubulins. The “input” is 10% of the MCF10A whole cell lysates used for the GST pull-down. MCF10A cells were either untreated (-Noc) or treated with nocodazole (+Noc) prior to lysate collection. (B) CHFR interacts with α tubulin by co-immunoprecipitation. A Flag:CHFR construct was transfected into HEK293 cells and the lysates were used for immunoprecipitation with either anti-Flag or anti- α tubulin mouse antibodies then Western blotted (WB) with either anti-Flag or anti- α tubulin rabbit antibodies. Cells were either untreated or treated with nocodazole. The “input” indicates 5% of the lysates used for the IP reaction. (C) CHFR ubiquitinates α -tubulin in nocodazole treated cells. MCF10A cells were cultured in MG132 and either untreated or simultaneously treated with nocodazole. Western blotting of immunoprecipitated α -tubulin for ubiquitin shows that the amount of ubiquitinated α -tubulin is dramatically decreased in MCF10A:CHFR-siRNA cells treated with nocodazole. The “input” indicates 10% of the lysates used for the IP reaction. (D) Western blotting reveals that MCF10A:CHFR-siRNA cells have a modest increase in unmodified and acetylated α -tubulin protein levels compared to control cells. (E) A graphic representation of the data presented in (D) from triplicate experiments.

Figure 5: A proposed model of how CHFR regulates genomic instability.

Decreased or lost CHFR expression causes Aurora A, α -tubulin, and acetylated α Tubulin over-expression and MAD2 mis-localization. The increase in acetylated α -tubulin occurs by an unknown mechanism, possibly through HURP or SIRT2 and may stress the mitotic spindle. Aurora A over-expression causes centrosome amplification. Both Aurora A over-expression and MAD2 mis-localization result in an impaired spindle checkpoint, contributing to aneuploidy and/or failed cytokinesis. Both processes lead to mitotic defects causing genomic instability, and possibly tumorigenesis.

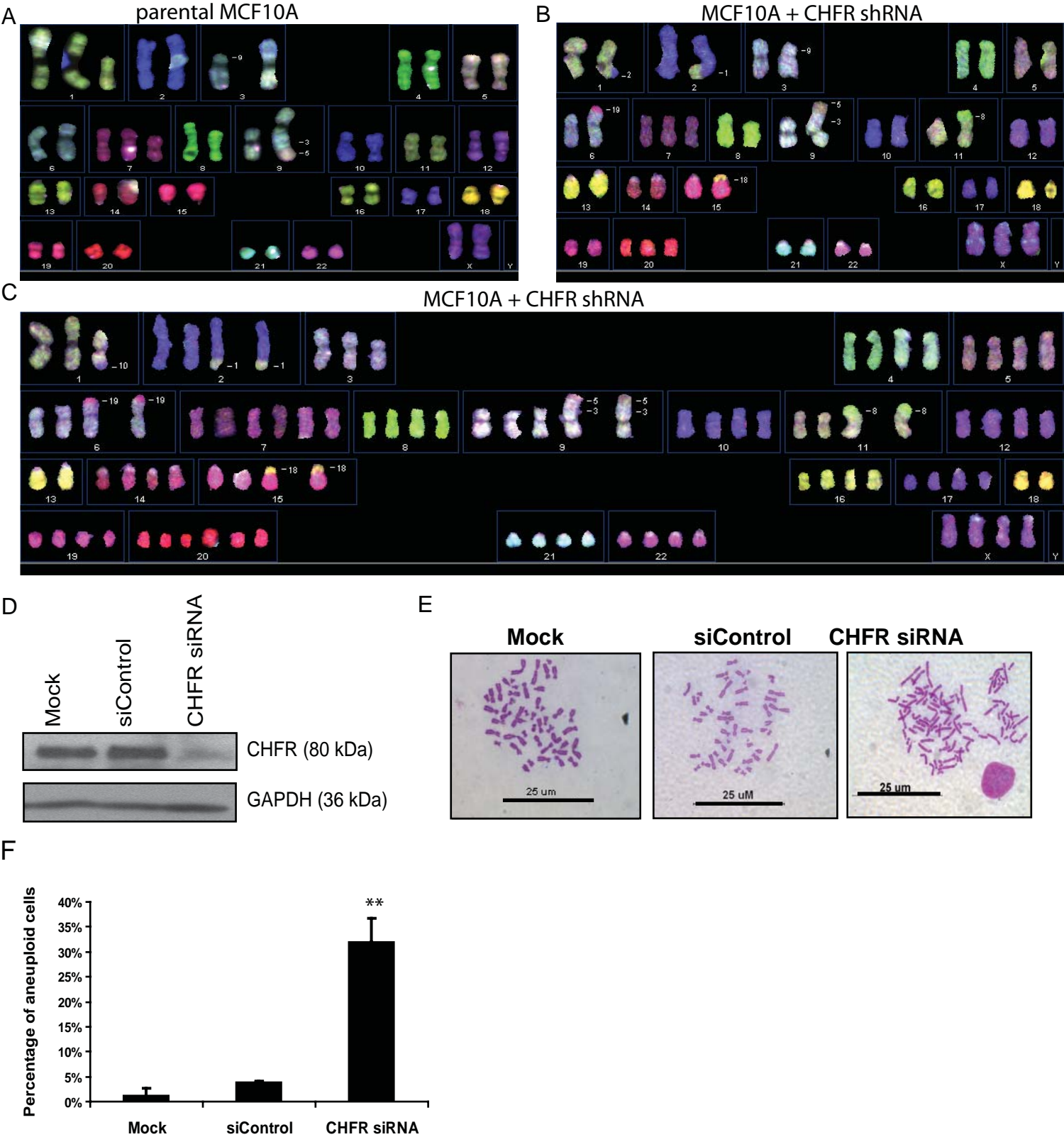


Figure 1
Privette

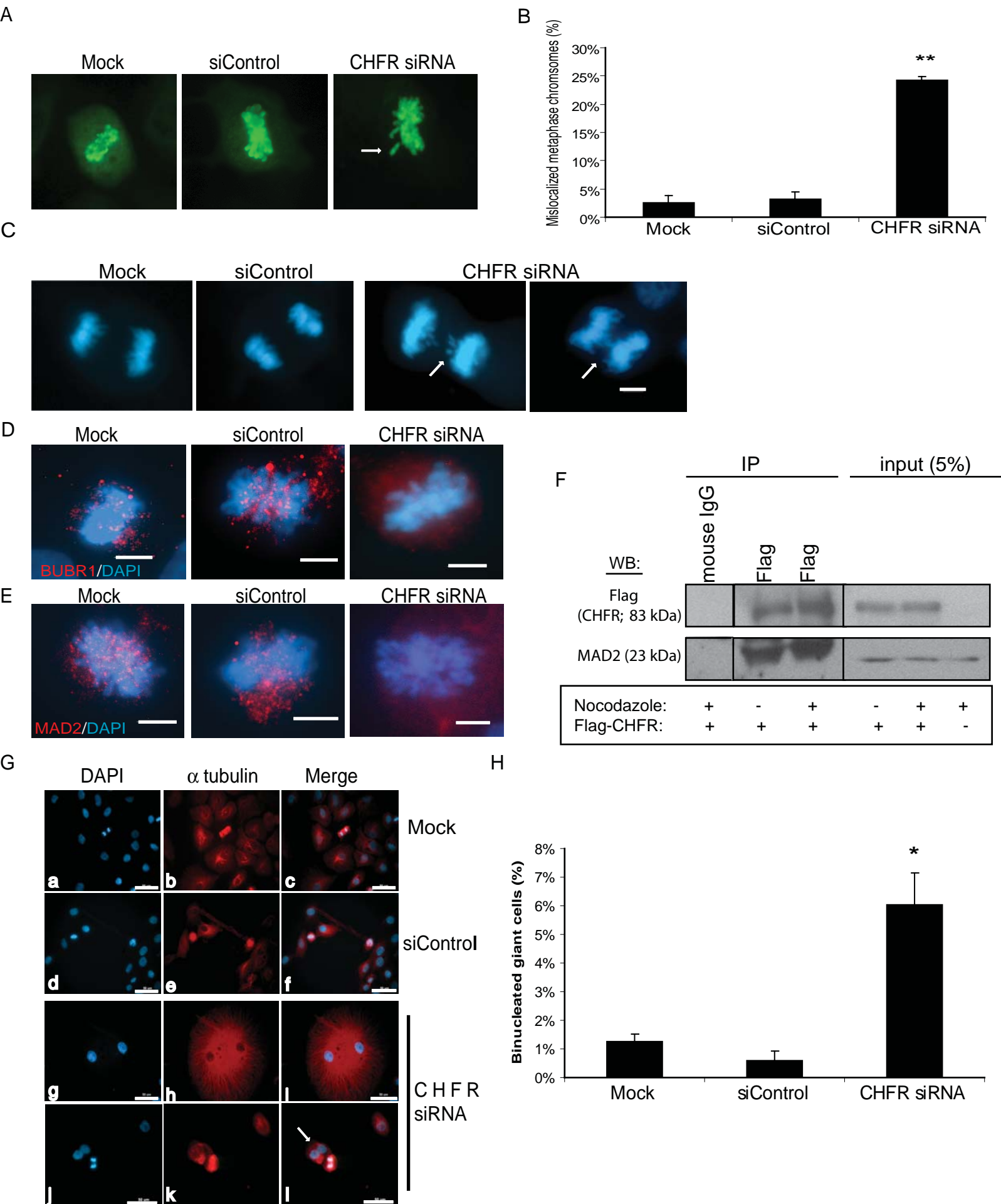


Figure 2
Privette

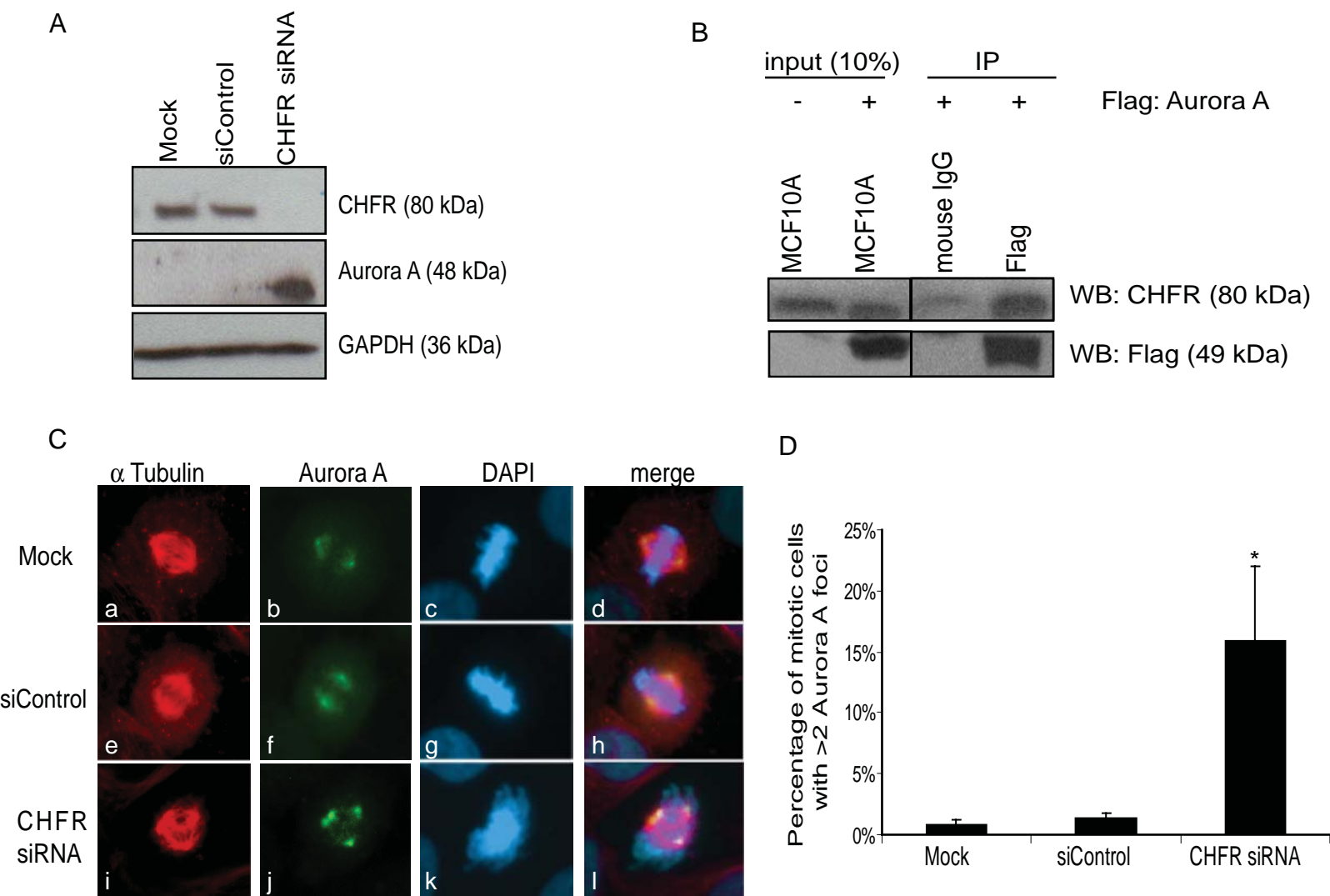
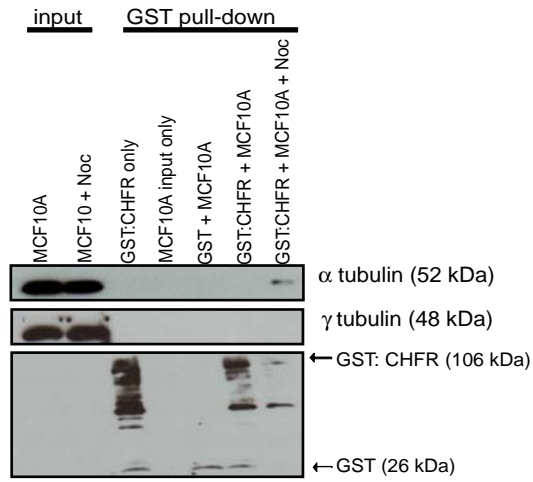
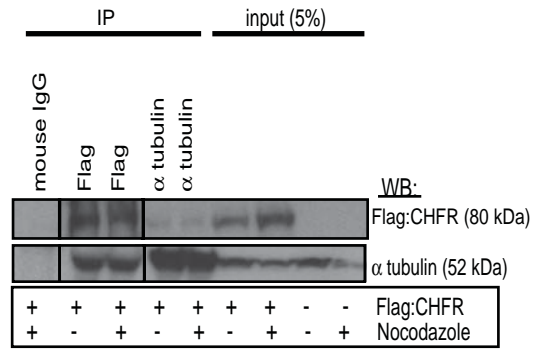


Figure 3
Privette

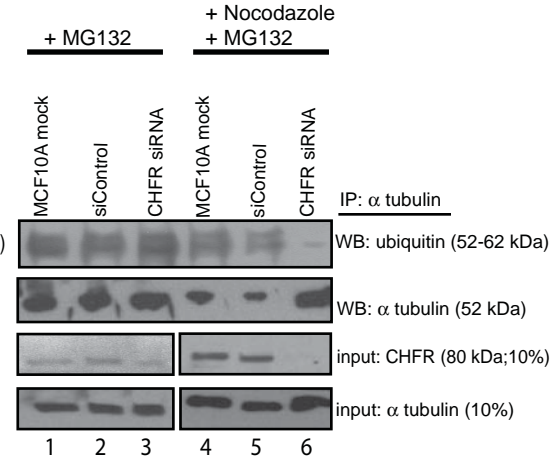
A



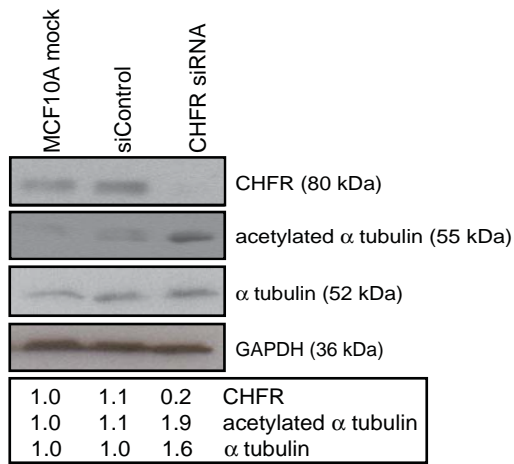
B



C



D



E

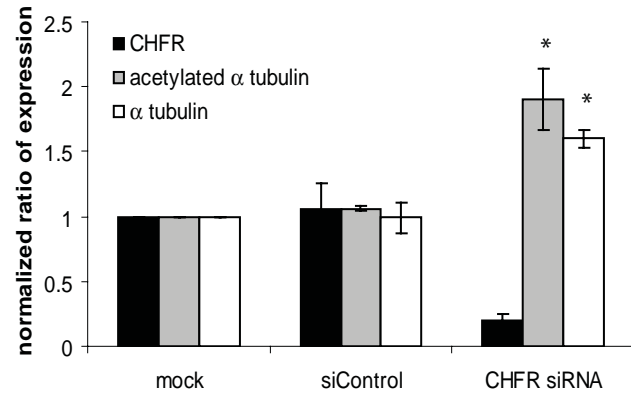


Figure 4
Privette

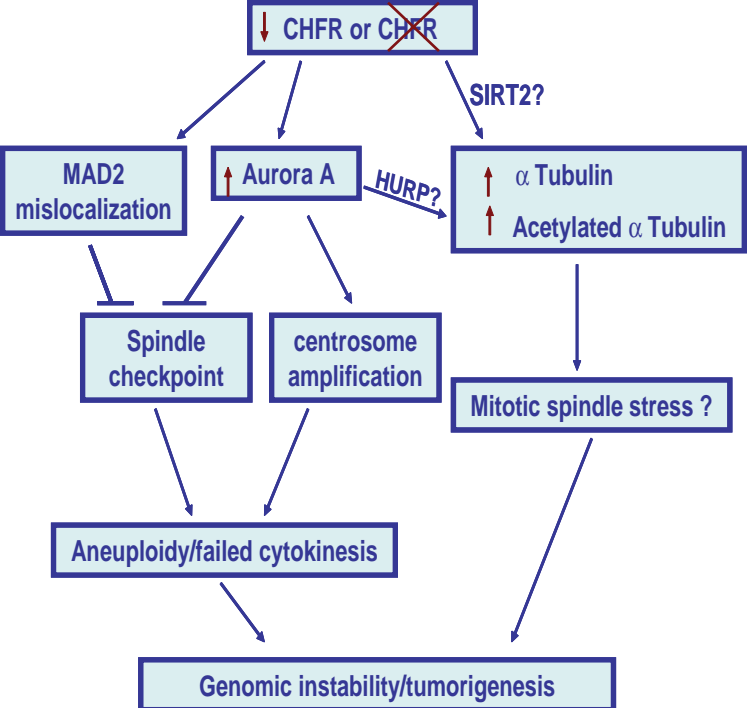


Figure 5
Privette

Lisa Marie Privette, M.S.

Campus Address:

1008 Island Drive Ct, #109
Ann Arbor, MI 48105
(513)543-8204
email: lprivet@umich.edu

Permanent Address:

486 Christina Dr.
Hamilton, OH 45013
(513) 867-0460

Education:

University of Michigan, Rackham Graduate School, Ann Arbor, MI

Ph.D. in Human Genetics

Degree conferred: April 25, 2008

Thesis Defense: February 1, 2008

Ph.D. Candidate (Candidacy Achieved 2004)

Masters of Science degree, awarded 2004

Department of Human Genetics (2003-present)

Program in Biomedical Sciences (2002-2003)

GPA: 8.103 / 9.0 (2002 - present)

Miami University, College of Arts and Science, Oxford, Ohio

Bachelor of Arts in Microbiology, May 2002

Bachelor of Arts in Classical Humanities, May 2002

Minor: Molecular Biology

Thematic Sequence in "Chemistry of Life Processes"

Cumulative GPA: 3.97/4.0

Honors and Awards:

University of Michigan

Department of Defense Breast Cancer Research Program Pre-doctoral Traineeship

- \$30,000/year for 3 yrs (Feb. 2006 – Jan. 2009)

Excellence in Teaching Award for graduate students, UM Medical School (Sep. 2007)

James V. Neel Fellowship in Human Genetics, Honorable Mention, May 17, 2007

University of Michigan Genetics Training Grant (2003-2005)

- Full funding of stipend, tuition, and health insurance
- Student Representative to the Executive Committee
- Course organizer, "Genetics of Host-Pathogen Interactions"

Miller Brewing Company Graduate School Merit Scholarship (2002-2006)

UM Department of Human Genetics Cramer Research Award (2004)

National Science Foundation Graduate Research Fellowship Honorable Mention (2003)

Miami University

summa cum laude

University Honors Program – graduated with University Honors

Department of Microbiology – graduated with Department Honors

President's List (1999-2000)

Dean's List (1998; 2000-2002)

Scholarships

- Miller Brewing Company Merit Scholarship
- Miami University Edward and Mary Rue Shepherd Alumni Merit Scholarship
- Hamilton Community Foundation, Jean & William Wolf Memorial Scholarship

- Bishop-Elliott Prize in Classical Humanities (2002)
 - Dr. J.K. Bhattacharjee Microbiology Award (2001-2002)
 - Orton K. Stark Microbiology Award (2000-2001)
- Miami MED Pre-Medical Honorary, member (1999-2002)
 The National Society of Collegiate Scholars, member (2000)
 The Golden Key International Honor Society (2000-2002)
 Phi Eta Sigma/Alpha Lambda Delta National Honorary, member (1999)

Activities:

University of Michigan

Department of Human Genetics

- Student Representative to the Faculty (2006)
- Admissions Committee (2005)
- Special Events Committee (2004, 2007)

Host student for Program in Biomedical Sciences applicants (2004-2007)

University of Michigan Life Sciences Orchestra, (2002-2005)

Miami University

Microbiology Club

- Treasurer (2000-2002)
- Member (1998-2002)

Teaching Experience:

Summer Science Academy (2003-present)

- Director of Genetics Laboratory Education, 70-80 hrs/year, (Jan. 2005-present)
- Genetics Lab Instructor, 14 hours (2003, 2004)

Michigan Teaching Fellow, certified through:

“Preparing Future Faculty” Rackham Graduate School Seminar Series/Workshop (May 2007)

- Competitive application process; selected participant
- 10-day workshop (50 hrs) on teaching skills, syllabus preparation, and academic job searches

University of Michigan Department of Human Genetics/Genetic Counseling Program

- Tutor for “Molecular Genetics, HG541,” approx. 60 hours

Graduate Student Research Assistantship (August – December, 2005)

- Department of Human Genetics, “Molecular Genetics, HG541,” approx. 70 hrs.

University of Michigan Genetics Training Grant Short Course (Sept. 2004-April 2005)

- Course Director, *The Genetics of Host-Pathogen Interactions*, approx. 25 hours

University of Michigan Program in Biomedical Sciences (Sept. 2003 – Dec. 2003)

- Tutor for “Molecular Genetics, HG541,” approx. 40 hours

Women in Science and Engineering (WISE) Summer Camp (2003)

- Genetics Lab Instructor, 4 hours

Miami University Office of Learning Assistance (August 2001- December 2001)

- Science Tutor in Chemistry, Biology, and Physics; approx. 25 hours

Mentored Students

- Lesley Everett: September 2007 – December 2007. PIBS (PhD) rotation student
- Amy Gaviglio: September 2005 – April 2006. M.S. student in UM Department of Human Genetics. Currently a genetic counselor in Minneapolis, MN

Invited Lectures:

“Lab Etiquette” for University of Michigan’s MedSOAR (Medical Summer Opportunities for Apprenticeships in Research) program for undergraduates; June 5, 2007.

“Lab Etiquette” for University of Michigan’s MedSOAR (Medical Summer Opportunities for Apprenticeships in Research) program for undergraduates; June 6, 2006.

Research Projects:

University of Michigan, Dissertation Research

- Advisor: Elizabeth Petty, M.D.
- Model: Primary human breast cancer tissues and breast cancer cell lines
- The roles of CHFR in mammary tumorigenesis and genomic instability.

University of Michigan, Winter Rotation (2003)

- Advisor: Jeffrey Innis, MD, PhD
- Model: *M. musculus*
- The identification of target genes regulated by the HoxA13 transcription factor during limb formation.

University of Michigan Fall Rotation (2002)

- Advisor: Thomas Glover, PhD
- Model: HeLa cells and mouse ES cell lines
- Functional characterization of Rad51 for the maintenance of genomic stability at chromosomal fragile sites.

University of Michigan, Summer Rotation (2002)

- Advisor: Elizabeth Petty, M.D.
- Model: Human breast and ovarian cancer cell lines
- Expression profiles of *SMARCA1-1* in breast and ovarian cancer cells.

The Ohio State University Molecular Genetics Research Experience for Undergraduates (2001)

- Advisor: Paul Herman, PhD
- Model: *S. cerevisiae*
- The role of DOT6 and its homolog, DTH6, in the regulation of telomeric silencing.

Miami University Howard Hughes Internship/Undergraduate Independent Study (2000)

- Advisor: Gary Janssen, PhD
- Model: *E. coli*
- The identification of novel sequences that contribute to the regulation of translation initiation.

Professional Memberships:

American Society of Human Genetics, Trainee member (2005)

American Society for Microbiology, student member (1998-2002)

Local Poster Presentations:

University of Michigan Cancer Center Fall Research Symposium, November 16, 2007

University of Michigan Department of Human Genetics Annual Symposium, May 17, 2007

University of Michigan Genetics Training Grant Annual Symposium, May 7, 2007
University of Michigan Department of Internal Medicine Annual Symposium, May 4, 2007
University of Michigan Cancer Center Fall Research Symposium, November 17, 2006
University of Michigan Genetics Training Grant Annual Symposium, June 1, 2006
UM Department of Human Genetics, 50th Anniversary Symposium, May 26, 2006
University of Michigan Department of Internal Medicine Annual Symposium May 20, 2006
University of Michigan Cancer Center Fall Research Symposium, November 2005
University of Michigan Department of Human Genetics Fall Retreat, October 2005
University of Michigan Genetics Training Grant Annual Symposium, April 2005
University of Michigan Cancer Center Fall Research Symposium, November 19, 2004
University of Michigan Department of Human Genetics Fall Retreat, October 15, 2004
Miami University Undergraduate Research Conference, April 17, 2002
The Ohio State University, Molecular Genetics REU, Poster Session, Aug 16, 2001

Oral Presentations and Seminars:

UM Genetics Training Grant Student Seminar, January 9, 2007
UM Dept. of Human Genetics Student Seminar, December 8, 2006
UM Dept. of Human Genetics, Annual Retreat, September 29, 2006
UM Dept. of Human Genetics Student Seminar, January 20, 2006
Miami University Undergraduate Seminar, October 9, 2001

Abstracts at National Meetings:

L.M. Privette and E.M. Petty, "Loss of CHFR potentiates the development of oncogenic phenotypes and creates genomic instability in mammary epithelial cells," "Mechanisms and Models of Cancer" meeting, Salk Institute, La Jolla, CA, August 8-12, 2007

M.E. Gonzalez, E.A. Peterson, *L.M. Privette*, J.L. Loffreda-Wren, L.M. Kalikin, and E.M. Petty, "*Sept9_v1* over-expression in human mammary epithelial models is associated with pro-oncogenic phenotypes," "Mechanisms and Models of Cancer" meeting, Cold Spring Harbor Laboratory, NY, August 16-20, 2006

L.M. Privette, M.E. Gonzalez, E.M. Petty, "Altered expression of the early mitotic checkpoint gene, *CHFR*, in breast cancer cells: Implications for tumor suppression," The Cell Cycle" meeting, Cold Spring Harbor, NY, May 17-21, 2006

L.M. Privette, M.E. Gonzalez, A.E. Erson, E.M. Petty, "Altered Expression of the Early Mitotic Checkpoint Gene *CHFR* in Breast Cancers: Implications for Tumor Suppression," ASHG 55th Annual Meeting, Salt Lake City, UT, October 25-29, 2005

E.M. Petty, M.E. Gonzalez, *L.M. Privette*, E.A. Peterson, J.L. Loffreda-Wren, "Analysis of a human septin gene, *SEPT_v1*, in mammary cells suggests novel oncogenic properties," ASHG 55th Annual Meeting, Salt Lake City, UT, October 25-29, 2005

Publications:

Privette, L.M. and Petty, E.M., "CHFR: a novel mitotic checkpoint protein and regulator of tumorigenesis," invited review, *in preparation for Histology and Histopathology*

Privette, L.M., Weier, J.F., Nguyen, H.N., Petty, E.M., "Loss of CHFR expression in mammary epithelial cells causes genomic instability" *submitted to Neoplasia*

Gonzalez, M.E., Privette, L.M., Petty, E.M., "SEPT9_v1 stabilizes JNK and contributes to its proliferative effects in mammary epithelial cells," *in preparation*.

Gonzalez, M.E., Peterson, E.A., Privette, L.M., Loffreda-Wren, J.L., Kalikin, L.M., Petty, E.M., "High *SEPT9_v1* expression in human breast cancer cells is associated with oncogenic phenotypes," *Cancer Res.* 2007; 67: (18). September 15, 2007

Privette, L.M., Gonzalez, M.E., Ding, L., Kleer, C.G., Petty, E.M., "Altered expression of the early mitotic checkpoint gene, CHFR, in breast cancers: Implications for tumor suppression," *Cancer Res.* 2007; 67: (13). July 1, 2007

Miami University Honors Thesis: Privette L.M. "The Effects of DOT6 and DTH6 on Telomeric Silencing and Cell Viability," Miami University Honors Department. April 2002

References:

Elizabeth Petty, M.D.

Associate Dean of Student Programs, UM Medical School
Professor, Departments of Internal Medicine (Division: MMG) and Human Genetics
5220 MSRB III
1150 West Medical Center Drive
Ann Arbor, MI 48109-0640
Phone: (734) 763-2532
Email: epetty@umich.edu

Sally A. Camper

Chair and Professor of Human Genetics
4909 Buhl
1214 East Catherine St
Ann Arbor, MI 48109
Phone: 734 763-0682
Email: scamper@umich.edu

Diane Robins, Ph.D

Professor, Department of Human Genetics
4909 Buhl
1214 East Catherine St
Ann Arbor, MI 48109
Phone: 734 764-4563
Email: drobins@umich.edu

Thomas Glover, Ph.D.

Professor, Departments of Human Genetics and Pediatrics & Comm. Diseases
4909 Buhl
1214 East Catherine St.
Ann Arbor, MI 48109
Phone: 734 763-5222
Email: glover@umich.edu

Additional references available upon request.